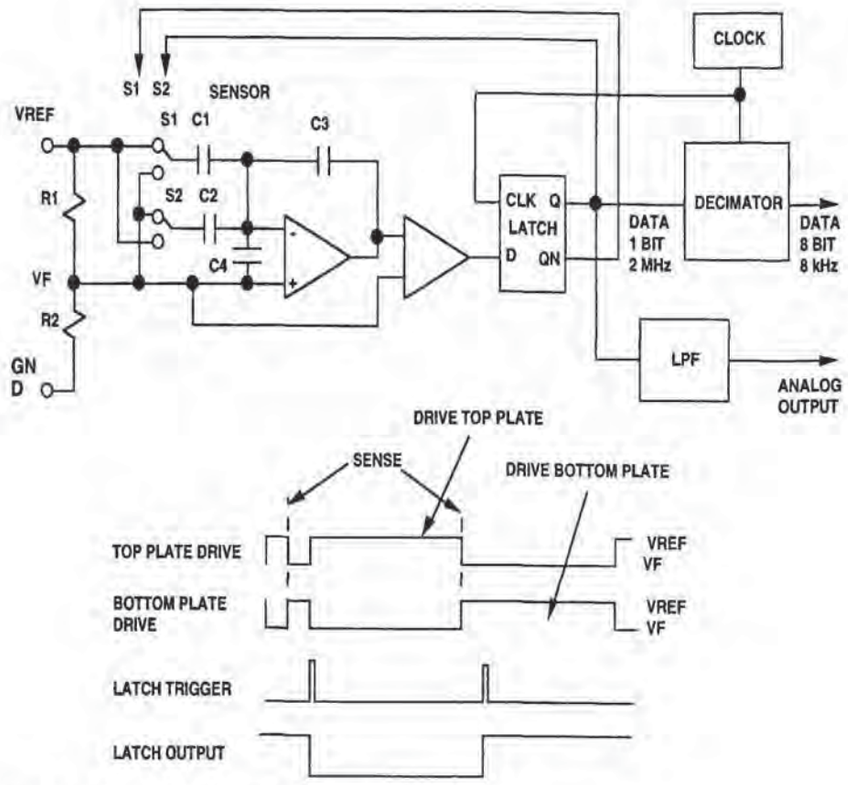


FIGURE 7.19 *Block diagram of Delta Sigma Modulator.*

accelerometers for the detection of side impact. This application will require additional air bags to the side of the occupants. Other low g linear accelerometers are being developed for ride control, ABS, traction, and inertial navigation applications.

Solid state acceleration sensors have special mounting requirements that are different from normal integrated circuits. These are to ensure that acceleration forces are transmitted to the sensor package. An advantage of the solid state device is self-test features for diagnostics. In acceleration applications, the devices are required to operate over the temperature range –40 to 85 °C (125 °C under the hood), and to withstand >2000 *g* shock. Other similar devices that have application in the automotive arena are vibration devices.

7.5.1 Air Bag Deployment Application

Crash sensors that use mechanical switches (sensors) are typically located some 40 cm from the point of impact, which necessitates the use of multiple sensors (normally 3 to 5 sensors are used in multipoint sensing) for crash sensing and air bag deployment. These devices are velocity change detectors, and are calibrated to make contact when the change of velocity in the passenger compartment is at least 20 km/h, this being the velocity change at which the front seat occupants will strike the windshield.

A centrally located analog sensor can be used as a crash sensor (single point). In the case of a centrally located accelerometer, the g level to be sensed is lower than that of a point-of-impact device. However, only one device is required to monitor the crash signature. This signature will vary with different types of chassis and different types of impacts. Consequently, an MCU is used to monitor the output of the accelerometer to determine if a crash has occurred. The typical output of a centrally located accelerometer during a 48 km/h crash is shown in Fig. 7.20. Deceleration of the vehicle and occupant displacement are also shown. At 48 km/h, the sensor has 20 ms to detect the crash and trigger the air bag. This results in infla-

PETITIONER'S EXHIBIT 1002
US PATENT NO. 6,557,540

tion of the air bag 50 ms after impact, at which time the occupant has moved about 18 cm or approximately halfway to the windshield and at the contact point with the inflated air bag. During the initial 20 ms, deceleration can reach 20 *g*, but the average is about 5 *g* when the air bag is triggered. The centrally located accelerometer can take one of several forms: a piezoelectric sensor, a piezoresistive device, or a capacitive sensor.

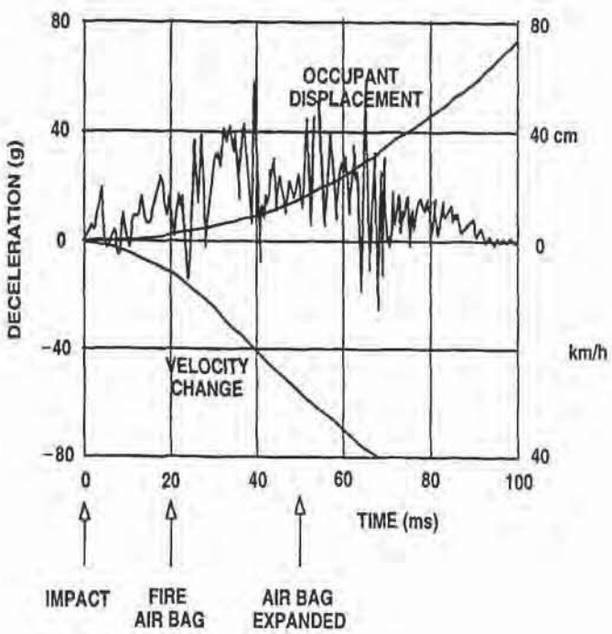


FIGURE 7.20 Typical 48 km/h crash waveform.

The centrally located accelerometer has a number of performance advantages over its mechanical counterpart. These are the reduction in the number of sensors and required bussing, which makes the centrally located system much more cost effective. There is an improvement in sensing and signal-processing accuracy with the single-point sensing accelerometer over the mechanical sensor. This gives a better-defined trigger point and overall improved performance across different chassis types. Capacitive sensors appear to have the edge in this application, because they have the potential of being cost effective, meet the requirements of the application, and have self-test features plus diagnostics available. In this application, a typical accelerometer specification is ±50 *g* full-scale output, accuracy ±5 percent over temperature, bandwidth dc to 750 Hz, and cross-axis sensitivity <3 percent. During impact, the crash sensor can also be used for seat belt locking.

7.5.2 Ride Control Application

In ride control systems, the leaf or coil springs located on the axles are replaced by four *wheel stations,* which form an active suspension. Each wheel station contains an oil-filled cylinder with a piston to set the distance of the frame above the axles and to isolate the frame from axle vibration. This is achieved using a servo feedback system. When a vehicle with conventional suspension encounters a foreign object on the highway, the load on the wheel increases as it moves up to negotiate the obstacle. This load increase makes the vehicle rise up. With a fully active suspension, the increase in load is detected and a servo valve is opened to transfer the necessary amount of oil from the appropriate cylinder to a storage container. Consequently, the load exerted on the chassis by each wheel is maintained at its specific level and

PETITIONER'S EXHIBIT 1002
US PATENT NO. 6,557,540

the chassis remains at its static level. After the object has been traversed, oil is pumped back into the cylinder to reestablish the static load conditions.

An alternative to the active suspension is the adaptive suspension system. In this case, information from the front wheels is gathered and used to predict road conditions for the control of the rear wheels. The advantage over the fully active suspension is one of cost, as the number of acceleration sensors is halved. During cornering, oil is also pumped into the outside wheel cylinders to minimize roll angle.[7]

A combination of sensors is used for active suspension. These are accelerometers, wheel speed sensors, chassis-to-ground sensing, and piston-level sensing in the suspension system. The low g accelerometers used on the axles of the four wheels to detect the load changes on the wheels have the following specifications: ±2 *g* full-scale, accuracy ±5 percent over temperature, bandwidth dc to 10 Hz, and cross-axis sensitivity <3 percent. The acceleration information and data from the wheel speed sensors is used to provide the information necessary for the MCU to operate the servo control valves. Hall effect, MRE, and opto sensors have been used for monitoring the level of the pistons in the wheel stations cylinders.

7.5.3 Vibration Applications

Lean-burn engines are being developed for improved emission levels and for better fuel economy (10 to 15 percent improvement). NO_x emissions are greatly reduced to meet federal standards. Lean-burn engines use high stoichiometric ratios; 20:1 and higher are necessary. At these ratios, combustion becomes unstable and torque fluctuations large. Consequently, antiknock and vibration sensors are required to supply the information necessary to the MCU, so that it can adjust the injected fuel amount and ignition timing for stability over widely varying conditions.

There are two types of solid state sensors that can be used in this application: piezoelectric devices and capacitively coupled vibration sensors. A typical vibration sensor contains a number of fingers of varying length which vibrate at their resonant frequencies when those frequencies are encountered. The resonance is capacitively coupled to the sensing circuit, and the outputs as shown are obtained. Optical sensors have also been used as antiknock sensors. In this case, the ignition spectrum is monitored for the detection of misfiring or knocking. Vibration sensors can also be used for vibration monitoring in maintenance applications.

7.5.4 Antilock Brake System Applications

In antilock brake systems, speed sensors are attached to all wheels to determine wheel rotation speed and slip differential between wheels. VR devices, as well as Hall effect and MRE devices, can be used in this application, as zero speed sensing is not required. VR devices have been used and shown to be cost effective in this application, but Hall effect and MRE devices are now being designed into these systems. Pressure sensors are used to monitor brake fluid pressure, and an accelerometer or ground-speed sensor can be used to provide information on changes in the vehicular speed. Brake pedal position and brake fluid pressure information are also required for control. All of this information is fed to an MCU, which processes the data and adjusts the brake fluid pressure to each wheel for optimum braking. Many of the elements of the ABS system can be used for the detection of lateral slippage on high-speed cornering, and can be used for traction and the direction of power to the wheels. Traction control applies in particular to slippery surfaces and with four-wheel-drive vehicles. Additional information over that used in ABS systems is required by the MCU for ASR applications, such as engine speed and throttle angle. In this application, servo feedback to the throttle may also be necessary.

A more cost-effective, but less accurate, system for ABS and ASR is the adaptive control system in which accelerometers are normally used to measure deceleration when braking, and

PETITIONER'S EXHIBIT 1002
US PATENT NO. 6,557,540

acceleration when the throttle is opened. If skidding occurs during braking, the brake pressure is reduced and adjusted for maximum deceleration, or the throttle adjusted for maximum traction. Typical specifications for the accelerometer required in this application are: ±1 g full-scale output, accuracy ±5 percent over temperature, bandwidth 0.5 to 50 Hz, and cross-axis sensitivity <3 percent.

7.6 NEW SENSING DEVICES

New cost-effective sensors are continually being developed. The technology and cost are often pushed by the application and volume requirements of the automotive industry and federal mandates. Today's silicon sensors and control electronics are limited in operating temperature to 150 °C to ensure long life of the devices. This operational temperature is adequate for most applications, but higher temperature operation may be required for sensors mounted in the engine compartment. The limit on the operating temperature of silicon devices can be extended to between 200 and 250 °C by the use of special isolation techniques such as dielectric isolation (this operating temperature applies to surface micromachined devices). For higher-temperature operation, alternative materials such as GaAs or SiC are being developed, but the cost of these devices limits their use at present.

A list of semiconductor conductor materials and maximum practical operating temperatures is given in Table 7.3. Higher operating temperatures have been reported but with poor longevity.

TABLE 7.3 Device Operating Temperatures

Material	Maximum practical operating temperature, °C
Si	150
Si (dielectric iso.)	250
GaAs	300
AlGaAs	350
GaP	400
SiC	500

7.6.1 New Rotational Speed-Sensing Devices

A number of new devices are being investigated to detect magnetic fields. These are flux gate, Weigand effect, magnetic transistor, and magnetic diode. The magnetic transistor at present is showing the most promise. The device operates on a similar principle to the Hall effect device. That is, the current division between split collectors (bipolar) or split drains (MOS) can be changed by a magnetic field. This current differential can then be detected and amplified to give an output voltage proportional to magnetic field strength. These devices can use either majority or minority carriers, and can be either vertical or lateral bipolar or MOS devices. The magnetic transistor has the potential of higher sensitivity than the Hall effect device.

Figure 7.21 shows the cross section of a lateral PNP magnetic transistor. The current from each collector is equal until a magnetic field is applied perpendicular to the surface of the device. The magnetic field causes an imbalance of current between the two collectors. Sensitivities with this type of structure have been reported as being an order of magnitude greater than in the Hall effect device.[8] Magnetic transistors and diodes can be directly integrated with the signal-conditioning circuits, which could make them very cost effective in future applications. A comparison of the magnetic transistor to other practical devices is given in Table 7.2.

PETITIONER'S EXHIBIT 1002
US PATENT NO. 6,557,540

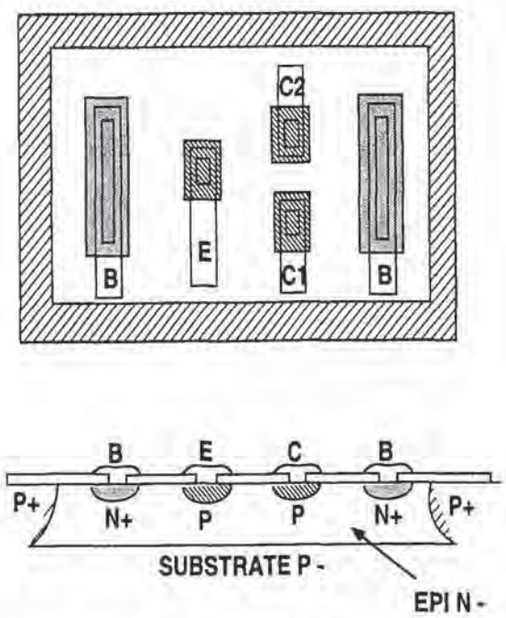


FIGURE 7.21 Cross section of a field-assisted *PNP* magnetic transistor.

7.6.2 New Linear Speed-Sensing Devices

A number of different sensing technologies can be used for distance, object detection, and approach speed measurements. Shown in Fig. 7.22 are the areas covered by blind-spot, rear, and forward-looking sensors. Ultrasonics, infrared, laser, and microwaves (radar) can be used in the detection of objects behind vehicles and in the blind areas. From a practical standpoint, no technology has come to the forefront. However, with new innovations in technology the situation may change very rapidly. Ultrasonics and infrared sensors are cost effective but degrade with inclement weather conditions such as ice, rain, snow, and the accumulation of road grime. Infrared devices are also color-sensitive, in that the sensitivity to shiny black objects is very low compared to other colors. Microwave devices appear to have the edge

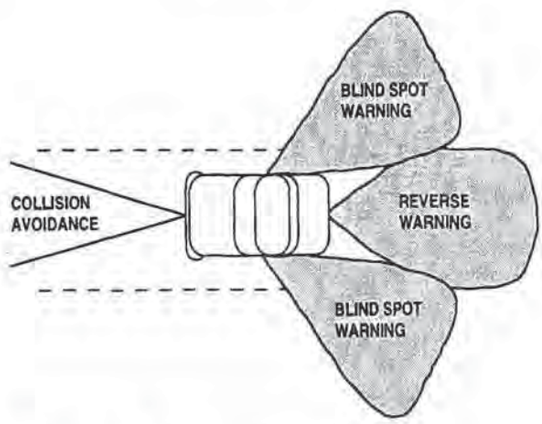


FIGURE 7.22 Collision-avoidance patterns.

PETITIONER'S EXHIBIT 1002
US PATENT NO. 6,557,540

when considering environmental conditions,[9] but are expensive, and radar can be affected by false return signals and clutter.

For the detection of obstacles and vehicles in front of a vehicle, the choice is between laser and microwaves due to the distances involved (up to 90 m). Microwaves have the disadvantage of high cost and large antenna size when considering available devices in the 60 GHz range. Frequencies greater than 100 GHz are preferred for acceptable antenna size. However, collision avoidance radar in the 76/77-GHz band has been developed in Europe. Collision avoidance radar in the 77, 94, and 144 GHz is being considered in the United States. A typical system uses a 38.5-GHz VCO (voltage controlled oscillator) with frequency-doubling to obtain about 40 mW of power at 77 GHz. A frequency-modulated continuous wave or pulse-modulated system can be used. The system uses GaAs devices to meet the frequency and power requirements. Lasers can be cost effective in this application, but also have their drawbacks: degradation of performance by fog, reflections from other light sources (sun, etc.), build-up of road grime on sensor surfaces, and poor reflecting surfaces at laser frequencies, such as grimy and shiny black surfaces.

7.6.3 New Inertial and Acceleration-Sensing Devices

Recent developments in solid state technology have made possible very small cost-effective devices to sense angular rotation. The implementation of one such gyroscopic device is shown in Fig. 7.23. This device is fabricated on a silicon substrate using surface micromachining techniques. In this case, three layers of polysilicon are used, with the first and third layers being fixed and the second layer free to vibrate about its center. The center is held in position by four spring arms attached to four mounting posts as shown. This device can sense rotation about the X and Y axes and sense acceleration in the direction of the Z axis. The center layer of polysilicon, driven by electrostatic forces, vibrates about the Z axis. These forces are produced by voltages applied between the fixed comb fingers and the comb fingers of the second polysilicon. Capacitor plates as shown are formed between the first and third polysilicon on the X and Y axes, and the second layer of polysilicon. Differential capacitive sensing techniques can then be used to sense any displacement of the vibrating disc caused by angular rotation. For example, if angular rotation takes place about the X axis, Coriolis forces produce a deflection of the disc about the Y axis. This deflection can be detected by the capacitor plates on the X axis. The sensing of the three functions is achieved by using a common sensing circuit that alternatively senses the X rotation, Y rotation, and acceleration. The gyroscope is designed to have a resolution of <10 degrees per hour for angular rate measurements, and an acceleration resolution of 0.5 mg.

7.7 FUTURE APPLICATIONS

New applications to increase creature comfort and safety are constantly being developed, but their rate of introduction will depend on the cost effectiveness of the technology, demand, and government mandates. Other concerns of automotive manufacturers are size, weight, power requirements, and adverse effects on styling and appearance. Many of the new sensor technologies are in their infancy, and thus are not yet cost effective on medium- and low-priced automobiles, but are being made available as options on luxury cars.

7.7.1 Future Rotational Speed-Sensing Applications

A future application for speed-sensing devices will be in continuously variable transmissions. In this application, engine and wheel speed, as well as torque, will be measured, and the infor-

PETITIONER'S EXHIBIT 1002
US PATENT NO. 6,557,540

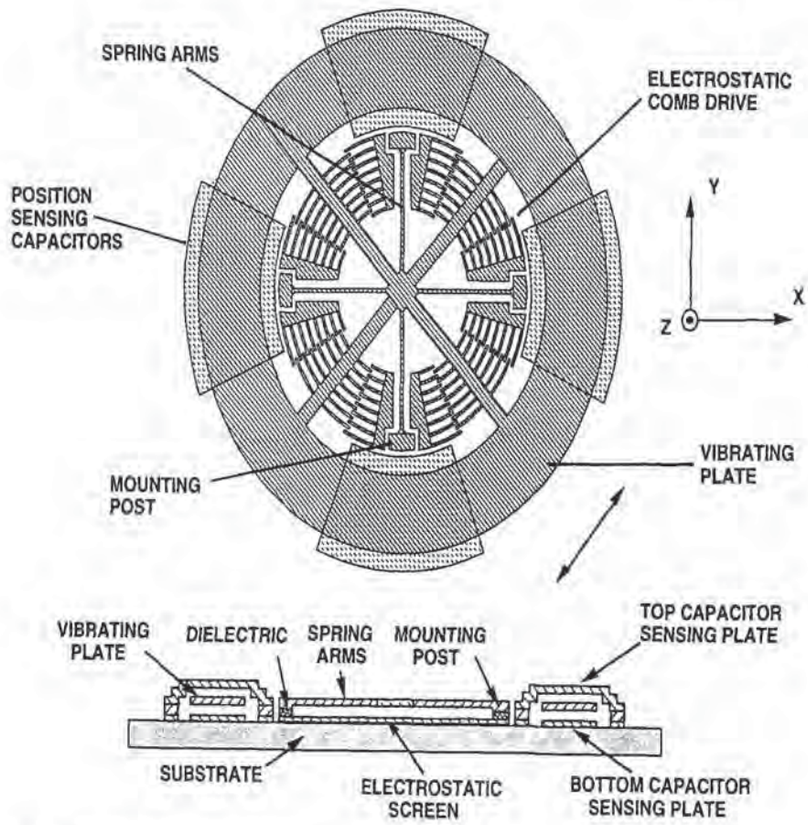


FIGURE 7.23 Solid state gyroscope.

mation processed by an MCU to optimize transmission ratios for engine performance and efficiency. All-wheel steering is also under development, and requires speed-sensing information, in addition to steering, front-, and rear-wheel angle position data for processing and control.

7.7.2 Future Linear Speed-Sensing Applications

Another application that has been developed is the use of speed- and distance-measuring devices for collision avoidance. These devices fall into three categories: near-obstacle detection (rear), blind-spot detection, and semiautomatic frontal object detection and control[9] (see Fig. 7.22).

Near-obstacle detection is used to prevent accidents during reversing. Blind-spot detection is used to prevent accidents due to careless lane changing, and when backing out of a driveway, garage, or alley into traffic. The semiautomatic frontal detection is a long-range system. The distance and closing speed between vehicles, or between a vehicle and a fixed object, can be measured and the speed adjusted as necessary to avoid a collision,[10] or the driver can be warned of impending danger. An addition to this is to monitor road surface conditions for friction—for example, dry roads compared to wet or icy roads—and also to use this information to adjust approach speeds and distance. Without collision avoidance, road condition monitoring can be used to caution vehicle operators. Collision avoidance systems can be used to minimize collisions, or can be used to operate protection systems before an unavoidable collision happens to protect the automobile passengers. In this case, vehicles closing at or approaching an obstacle at 80 km/h will be less than 7 m apart before a collision-is-imminent

PETITIONER'S EXHIBIT 1002
US PATENT NO. 6,557,540

determination can be made. This gives 200 ms decision-making time for the system MCU. This is, however, long compared to today's air bag deployment systems, which have 20 ms decision-making time after the event. In the future, an idealistic system may be a combination of the two systems.

7.7.3 Future Acceleration Applications

One of the future applications being considered is the expansion of the air bag system to include side impact protection. The sensor used for crash sensing is unidirectional, so that it can only detect forward impact. A similar sensor, mounted perpendicular to the air bag sensor, can be added to the system to detect side impact and to deploy protection for the passengers. This device will typically require a 250-*g* accelerometer. Another application for accelerometers is to detect slippage during cornering in advanced steering systems. These systems will employ a low-*g* accelerometer (1–2 *g*).

7.7.4 Inertial Navigation Applications

A number of inertial navigation systems are being developed for short- and long-range travel. Long-range inertial navigation systems normally obtain their location by using a triangulation method. This method references three navigation satellites with known locations in fixed orbits. However, there are certain conditions under which contact with all three satellites is lost. This occurs when the vehicle is in the shadow of tall buildings or high hills, and triangulation is not possible. Under these conditions, the guidance system has to rely on such devices as gyroscopes, which sense angular rotation or change in direction, and/or monitor vehicular motion relative to the road.

Short-range inertial navigation systems or inertial measurement units (IMU) rely to a large extent on high-accuracy accelerometers and gyroscopes. A typical accelerometer specification for this application is: ±2-*g* full-scale output, accuracy 0.5 percent over temperature, bandwidth dc to 20 Hz, and a cross-axis sensitivity <0.5 percent. A centrally located IMU can be expanded to cover other applications such as suspension, ABS, ASR, and working with crash avoidance sensors. This may be the way to handle cost-effective system design in the future. The IMU can also be designed to provide location data for intelligent vehicle highway systems. These systems (Prometheus,[11] Amtics[12]) improve travel efficiency and reduce fuel consumption and pollution by selecting the optimum route to a given destination. The route is chosen to avoid traffic congestion, road construction, and accidents (see Chap. 29).

7.8 SUMMARY

In this chapter, a number of speed-sensing devices, both rotary and linear, have been described, together with potential applications. VR, MRE, Hall effect, and opto devices (possibly magnetic transistor in future applications) can be used in rotational applications for engine control, transmission, and wheel speed sensing. Of these devices, Hall effect, VR, and opto have been widely used. With the tendency for direct pickoff, optical devices may become impractical. MRE devices are being designed in and will become a serious contender to the Hall effect device. In linear applications for crash avoidance, microwave devices have the edge over performance and optical devices in terms of cost. However, as the cost of microwave devices declines, they could become cost effective. For blind-area alert and reversing obstacle detection, ultrasonics and infrared devices are cost effective, but performance degrades during inclement weather.

PETITIONER'S EXHIBIT 1002
US PATENT NO. 6,557,540

The accelerometer has possibly the greatest potential for applications in the automobile. These applications range from crash sensing, ride control, ABS, and ASR to IMU systems. Accelerometers needed will range in sensitivities from 50 *g* in crash sensing to 1 *g* in the IMU. Advances in technology are providing a number of new sensors that are showing potential, such as the magneto transistor and the micromachined gyroscope. To summarize, Figs. 7.24 and 7.25 show the types of sensors used in specific applications, and the technologies used for specific sensors. As can be seen, one type of sensor can be used in a number of applications. In applications where a sensor output is shared, care must be taken to ensure that a failure in one system does not disable the sensor or other systems. Because of the similarities in several of the systems and the use of shared sensors, the greatest potential for cost-effective system design is a single control system. The IMU shows great potential to be the controller for ride control, ABS, ASR, four-wheel-drive, and steering applications. The rate of introduction of new sensors and systems will depend on federal mandates, customer demand, and the need to improve engine fuel efficiency and to reduce emissions.

GLOSSARY

Adaptive suspension A suspension system that monitors motion of the front wheels and adjusts the suspension of the rear axle accordingly.

Arntics Acronym for Advanced Mobile Traffic Information and Communication System.

ASR (traction) A system to prevent wheel spin on slippery surfaces, to give maximum traction and acceleration.

Sensor / Application	Air Bag Deployment	Ride Control	ABS	Engine Control	Transmission	4 Wheel Drive	All Wheel Stearing	Engine Vibrarion	Cruise Control	Seat Belts	Power Steering Assist	Traction (ASR)	Collision Avoidance	Obstacle Detection	Inertial Navigation
Speed Rotation	■	■	■	■	■	■	■		■		■	■			
Speed Linear			□		□				□		□	□	□	□	□
Acceleration	■	■	■	■						■		■			■
Vibration								■							
Angular Rotation															■

■ USED □ MAY BE USED

FIGURE 7.24 Sensor applications.

PETITIONER'S EXHIBIT 1002
US PATENT NO. 6,557,540

Measurand / Sensing Technique	Mechanical	Piezoelectric	Piezoresistive	Capacitive	Optical	Infrared	Radar	Laser	Ultrasonic	Hall Effect	Variable Reluctance	Magnetoresistive
Speed Rotation					☒					☒	☒	☒
Speed Linear						☒	☒	☒	☒			
Acceleration	☒	☒	☒	☒								
Vibration		☒		☒								
Angular Rotation				☒								

FIGURE 7.25 Sensor technologies.

Coriolis forces Forces exerted by a spinning body to oppose any motion at right angles to the axle.

Crash signature Shock waveform projected through a chassis during a collision.

Inertial navigation Guidance system giving accurate location.

IMU (inertial measurement unit) System used for guidance between two locations indicates road hazards and delays.

Lean burn Engine with high compression ratios and high air-to-fuel ratios for increased efficiency and low emissions.

Micromachining Manufacturing technology for micromechanical structures using chemical etching techniques.

NO_x Chemical symbol for oxides of nitrogen.

Prometheus Acronym for PROgraM for a European Traffic with Highest Efficiency and Unprecedented Safety.

Switched capacitor filter Technique for switching capacitors to simulate high-value resistors for low-frequency filters to minimize size.

REFERENCES

1. Osamu Ina, Yoshimi Yoshino, and Makio Lida, "Recent Intelligent Sensor Technology in Japan," S.A.E. paper 891709, 1989.
2. D. E. Bergfried, Mattes, B., and Rutz, R., "Electronic Crash Sensors for Restraint Systems," *Proceedings of the International Congress on Transportation Electronics,* Detroit, Oct. 1990, pp. 169–177.

PETITIONER'S EXHIBIT 1002
US PATENT NO. 6,557,540

3. E. Peeters, Vergote, S., Puers, B., and Sansen, W., "A Highly Symmetrical Capacitive Microaccelerometer with Single Degree of Freedom Response," *Tranducers 91,* 1991, pp. 97–103.
4. J. T. Suminto, "A Simple High Performance Piezoresistive Accelerometer," *Transducers 91,* 1991, pp. 104–107.
5. J. C. Cole, "A New Capacitive Technology for Low-Cost Accelerometer Applications," *Sensors Expo. International,* 1989.
6. T. A. Core, Tsang, W. K., and Sherman, S. J., "Fabrication Technology for an Integrated Surface-Micromachined Sensor," *Solid State Technology,* Oct. 1993, pp. 39–47.
7. H. Wallentowitz, "Scope for the Integration of Powertrain and Chassis Control Systems: Traction Control—All Wheel Drive—Active Suspension," *Proceedings of the International Conference on Transportation Electronics,* S.A.E. paper 901168, 1990.
8. H. Kaneko, Muro, H., and French, P. J., "Optimization of Bipolar Magneto-Transistors," *Micro Systems Technologies 90,* 1990, pp. 599–604.
9. L. Raffaelli, Stewart, E., Borelli, J., and Quimby, R., "Monolithic Components for 77 GHz Automotive Collision Avoidance Radars," *Proceedings Sensors Expo,* 1993, pp. 261–268.
10. S. Aono, "Electronic Applications for Enhancing Automotive Safety," *Proceedings of the International Conference on Transportation Electronics,* SAE 901137, 1990, pp. 179–186.
11. J. Hellaker, "Prometheus-Strategy," *Proceedings of the International Congress Transportation Electronics,* SAE 901139, 1990, pp. 195–200.
12. H. Okamoto, and Hase, M., "The Progress of Amtics-Advanced Mobile Traffic Information and Communication System," *Proceedings of the International Congress Transportation Electronics,* SAE 901142, 1990, pp. 217–224.

ABOUT THE AUTHOR

William C. Dunn is a member of the technical staff in the Advanced Custom Technologies group at Motorola's Semiconductor Product Sector in Phoenix, Arizona. He has over 30 years' experience in circuit design and systems engineering. For the past 15 years he has been involved in the development of semiconductor sensors, smart power devices, and control systems for the automotive market. Prior to joining Motorola, he worked for several large corporations in the United Kingdom and United States, has written over 30 papers, and has over 30 patents issued and pending on mechanical sensor structures, semiconductor technology, and circuit design.

PETITIONER'S EXHIBIT 1002
US PATENT NO. 6,557,540

PETITIONER'S EXHIBIT 1002
US PATENT NO. 6,557,540

CHAPTER 8
ENGINE KNOCK SENSORS

William G. Wolber
Executive Engineer
Cummins Electronics Co., Inc.

8.1 INTRODUCTION

Knock is a phenomenon characterized by undesirable structural vibration and noise generation and is peculiar to spark-ignited engines. Knock is undesirable both from a customer acceptance standpoint and also because severe knock can cause engine damage. The terms *ping* (light, barely observable knock) and *predetonation* (knock caused by ignition of the charge slightly before the full ignition of the flame front by the spark plug) are also commonly used in the industry, and not always with precision.

Historically, knock became an important engine phenomenon in the 1930s. In their search for performance improvements, designers of spark-ignited engines increased compression ratios beyond the capabilities of the gasoline formulations available to provide smooth, knock-free combustion. The discovery of gasoline additives such as tetraethyl lead, which improve the stability of the combustion process primarily by decreasing burn rate, permitted the fuel suppliers to provide a range of fuel knock properties at the pump to match with the range of engine requirements. As a result, by 1950, knock was not regarded as a significant engine performance limiting parameter since the car company could specify what fuel should be selected, ranging from "regular" to "super premium" grades. A blending fuel pump was even provided by one fuel company which allowed the operator of the vehicle to select exactly what grade of fuel he or she wished to use from a selection of six grades.

In the late 1960s, the situation began to change drastically. In response to public concern about air quality and health, legislation on automotive emissions became a new constraint on automotive engine design, first in the United States and more recently worldwide. The use of fuel additives to improve gasoline knock characteristics fell into disfavor for two reasons:

- Many of the better additives resulted in combustion products not desirable in the air. For example, most lead compounds are toxic at low levels to human and animal life.
- As engine designers strove to provide lower engine emissions, the use of the three-way catalytic converter cleanup device in the exhaust system became nearly universal. Unfortunately, most good fuel additives that improve knock characteristics poison the catalyst of the converter, rendering it ineffective. Also, many engine controls began to make use of the oxygen sensor feedback control loop. The catalyst on the oxygen sensor also is poisoned by the better additives.

This situation led to gradually more stringent federal regulation of the fuel industry, a trend which, in the end, legislated fuels with knock-improving additives completely off the

PETITIONER'S EXHIBIT 1002
US PATENT NO. 6,557,540

market, so that by the mid 1980s, all spark-ignited automobile engines in the United States were being operated using lead-free gasoline. Of course, as leaded gasoline disappeared, the knock phenomenon returned. The auto industry knew what to do—lower compression ratios—but this step alone has accompanying negative consequences, such as lower fuel economy. Thus, the situation was one driven by the need to optimize between several principal goals: emission regulations, fuel supply characteristics, fuel economy goals, customer acceptability, and vehicle performance.

8.2 THE KNOCK PHENOMENON

8.2.1 Definition

Spark-ignited engine knock has been defined as "an undesirable mode of combustion that originates spontaneously and sporadically in the engine, producing sharp pressure pulses associated with a vibratory movement of the charge and the characteristic sound from which the phenomenon derives its name."[1] This definition at once conveys some of the difficulties of measuring the phenomenon and devising engine controls to minimize it. First, the ultimate standard is the reaction of the human to the vibration felt or the sound heard as a result of the knock. An attempt to measure the cause of the phenomenon leads one to the difficult problem of observing pressure waves in the cylinder. In fact, over the years these difficulties led the industry to devise an experimental comparison measurement technique which measured the octane rating of the *fuel*, not of the engine.

8.2.2 Laboratory Measurements

The CFR Engine. The basic comparison method which evolved for rating fuel knock quality involved the use of a simple, single-cylinder, spark-ignited engine called the CFR engine, and a pure hydrocarbon fuel—100 percent isooctane. Researchers discovered that they could reproduce knock phenomenon, laboratory to laboratory, by running this engine under specified conditions with this fuel.

Gasoline Octane Rating. A system of rating the knock characteristics of fuels, called the octane rating, was developed based on a comparison of the CFR engine performance with the test fuel compared to pure isooctane. On this scale, osooctane has an octane rating of 100; passenger car engine fuels ranged from the high 70s for "regular" to the high 90s for "super premium." (Fuel formulations with an octane rating over 100 were possible but were used mainly for aircraft engines.)

As the industry strove to put knock on a solid engineering basis, methods of measuring the resulting phenomena on the CFR engine, and commercial engines as well, were developed. The parameter on which the industry standardized was "jerk," the third-time derivative of engine block displacement. Scales evolved for comparing the relative knock performance of fuels and of engines based on the output of this kind of sensor. Much work was also done to correlate jerk sensor measurements with cylinder pressure phenomena.

The fundamental resonant frequency of the knock-generated pressure signal is dependent on engine cylinder geometry and the speed of sound in the charge gas. The structural vibration characteristics of the engine block that are excited by the fundamental knock event are determined by the engine block transfer function. Testing conducted on one cylinder of a six-cylinder spark-ignited engine demonstrates that high-frequency structural vibration components are good indicators of knock, despite the relatively low frequency high-pressure excitation event.[2] Structural vibration induced by mechanical events, such as valves opening

PETITIONER'S EXHIBIT 1002
US PATENT NO. 6,557,540

and closing, introduces noise that can be confused with knock-induced vibrations. Careful signal analysis is required to overcome a sometimes poor signal-to-noise ratio.

The reverberation resonance of the cylinder typically lies in the range between 2 and 12 kHz. A useful rough estimate of the knock frequency for a given engine cylinder geometry is given by Draper's equation[3]:

$$\text{fr} = \frac{\text{Pmn} \times C}{\pi B} \tag{8.1}$$

where fr is the knock resonant frequency
Pmn is a vibration mode constant
C is the velocity of sound in the gas in the cylinder
and B is the radius of the cylinder

Using this equation, assuming that the average gas temperature is 2000 K so that C is 900 m/s, the first circumferential mode resonant frequency is estimated at 5.75 kHz for a cylinder of 10-cm bore.

As better cylinder pressure sensors have become available, cylinder pressure wave measurements, along with signal analysis techniques for deriving a knock rating number, have supplemented jerk measurements in the laboratory. The most popular signal analysis approach is to declare the maximum amplitude or peak-to-peak value of the bandpass filtered pressure data as a knock number, usually referred to as *knock intensity.*

Other ways of describing knock level are the root-mean square, mean square, or integral of the absolute value of the bandpass pressure oscillations during the knocking portions of the cycle. The spectral power of the pressure transformed into the frequency domain has been used for measurement. Derivative-based methods have also been established, based on rapid changes of cylinder pressure during the knock phenomenon, using the first, second, and third derivatives of the cylinder pressure history.

8.2.3 On-Board Knock Control

Improved Fuel Economy by Lowering Engine Compression Ratio. As engine control using microcomputers became established in the late 1970s and early 1980s for gasoline passenger car engines, and the octane rating of the fuels available for them dropped below 90, the automotive industry responded by lowering engine compression ratios. However, some of these smaller engines were equipped with turbochargers to recover some of the lost performance at wide open throttle. It was found that these engines could experience destructive high-speed knock at maximum speed and power. Not only were the knock reverberations in the cylinder large, but they were modulating a high base pressure wave. This could occur because the extra boost pressure from the turbocharger permits additional fuel to be metered to the engine without violating emissions restrictions on the control, since the amount of oxygen available to react with the fuel is greater. This could result in knock wave peaks exceeding the cylinder head pressure limit, as well as excessive vibration of the entire engine.

The knock occurring at wide open throttle had to be decreased, but retaining the additional power from the turbocharger at part throttle was very desirable. The electronic control was available to modulate the amount of fuel injected during the dangerous engine state; however, a means of sensing engine knock on-board in real time was needed. The sensors used are described in Sec. 8.3. The control operates by sensing that knock is over the permissible limit, and then reduces it either by retarding ignition timing or by opening a wastegate valve on the boosted manifold pressure.

Improved Fuel Economy by Raising Compression Ratio. Following the successful implementation of knock limit control on turbocharged engines, considerable experimentation was carried out to assess whether or not there is value in applying knock limit control to naturally aspirated spark-ignited engines. It was determined that if the engine knock was always kept

PETITIONER'S EXHIBIT 1002
US PATENT NO. 6,557,540

less than an empirically determined limit for that type of engine and stored in the microcomputer control memory, then the knock level would not be objectionable even to the more critical car operators. Moreover, this could be accomplished while raising the compression ratio one full number—for example, from 8:1 to 9:1. If used to improve fuel economy, this change results in a 3 percent improvement in the corporate average fleet economy (CAFE) rating for that model/engine combination. At today's CAFE values, this is close to a one-mile-per-gallon improvement.

CAFE values are extremely important to a passenger car original equipment manufacturer (OEM). The larger, heavier luxury cars cannot achieve as low a CAFE value as the smaller, lighter cars. However, the larger cars are more profitable to produce. Thus, the mix of cars produced by an OEM can depend on just how close his CAFE results are coming to the mandated value. A way of improving fuel economy without downsizing, adding significant cost, or losing performance is very valuable.

Starting in the early 1980s, more and more passenger cars had a knock limit control and increased compression ratio. Such a change is usually scheduled at a time when the engine design and the tooling to make the engine are changing for other reasons. By 1990, 25 to 30 percent of the naturally aspirated passenger car engines produced in the United States (and all of the turbocharged engines) featured knock limit control.

8.2.4 Measurement and Control System Considerations

In addition to the problem of developing a suitable on-board sensor for knock, once the parameter to use had been selected, a number of other considerations had to be settled in effecting a satisfactory control. It was already pointed out that engine knock can be reduced either by retarding spark timing or by opening a manifold boost wastegate valve. In the United States, the candidate engines already had electronic control of spark timing, so that all that was needed to implement the knock control was an easily added change in the timing command in the control microcomputer. However, many control strategies exist for processing the knock signal. Perhaps the most elaborate of these was implemented on the first turbocharged engine knock limit control:

- The vibration frequency of the knock is specific to the engine model but lies between 2 and 12 kHz for passenger car engines. The sensor used was mechanically bandpass-tuned to match this characteristic with a Q of about 2.
- The major knock reverberations for a given cylinder occur during a time window that starts shortly after the cylinder reaches top dead center and ends 60 to 90 crank-angle degrees later. The control opened a signal gate to allow the knock signal to pass through and be averaged only when the engine was in these time windows.
- To prevent engine damage, whenever the knock signature exceeded the limit value, the control very rapidly retarded ignition by as much as 10 crank-angle degrees so that the engine would not be in severe knock even for the next few cylinder events. Then the control would very slowly advance the timing until the process repeated. This resulted in somewhat less than best engine performance but assured a comfortable margin of safety for the engine.
- The knock threshold limit in the control was modulated to increase with engine speed so as to compensate for greater noise background at high engine speed.

8.3 TECHNOLOGIES FOR SENSING KNOCK

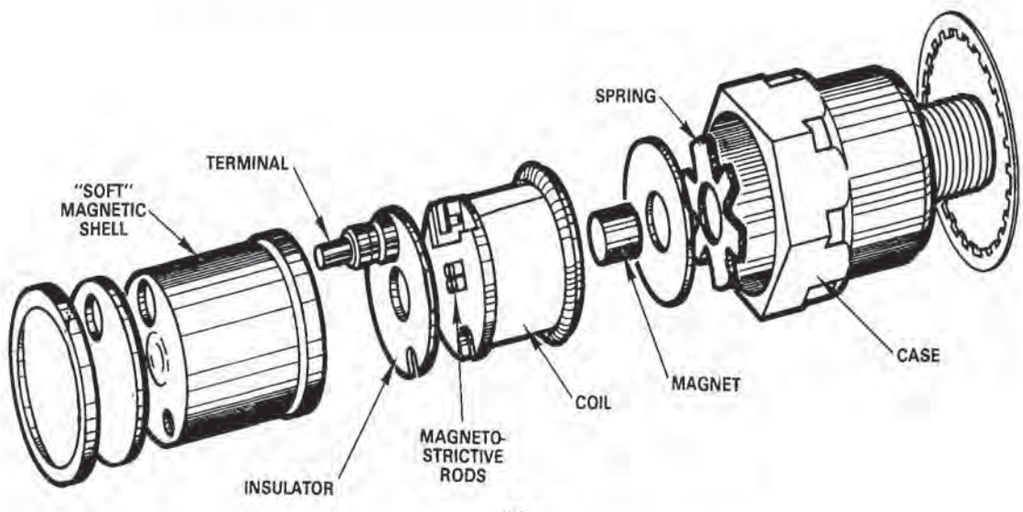
A number of different parameters have been selected for measuring knock in real time on board, and sensors have been developed for this purpose. It must be recognized that these

PETITIONER'S EXHIBIT 1002
US PATENT NO. 6,557,540

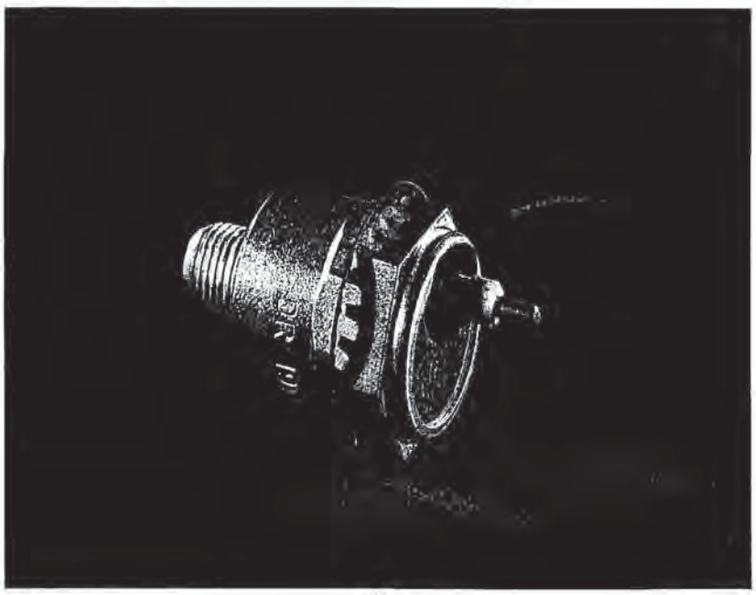
sensors measure the magnitude of a consequential parameter driven by the knock, rather than the knock phenomenon itself. The overall effectiveness of the control is therefore determined not only by the intrinsic performance and stability of the sensor and control, but also by how robust the chain of causality is between the knock phenomenon and the parameter measured.

8.3.1 Jerk Sensors

Naturally enough, the first turbocharged engine knock limit control used a jerk sensor, a productionized version of the kind of sensor used for laboratory CFR engine testing. An exploded view of this sensor is shown in Fig. 8.1.



(a)



(b)

FIGURE 8.1 (*a*) An exploded view of a jerk sensor, and (*b*) a photograph of the sensor.

PETITIONER'S EXHIBIT 1002
US PATENT NO. 6,557,540

Referring to the exploded view, it must be understood that when the sensor is fully assembled, the spider spring is preloaded, and all parts of the sensor except the coil cover are in compression. The nickel alloy magnetostrictive rods are biased mechanically in lengthwise compression and magnetically by the field impressed through the rods from the permanent magnet, returning through the ferromagnetic soft iron coil cover. The nickel alloy rods are the highest reluctance element in this magnetic circuit, and are in magnetic saturation.

The vibrations which are picked up and transmitted from the engine block through the mounting stud appear in the nickel alloy rods. These rods are of such a length that they comprise a broad passband mechanically resonant element. The compressive mechanical bias is sufficiently strong that the compression and rarefraction waves picked up are never large enough to take the rods out of net compression. The waves present in the rods therefore linearly modulate the magnetic reluctance of the magnetic circuit.

The many-turn coil wound around the magnetostrictive rods generates a voltage proportional to the rate of change of the magnetic flux; the flux, in turn, is inversely proportional to the magnetic reluctance of the rods. Since the vibrations picked up are already due to accelerations from the knock reverberations transmitted through the engine block, the voltage from the coil represents the third-time derivative of displacement, or jerk.

The vibration signal from a knocking engine is present virtually everywhere on the engine block, with signals from all cylinders superimposed. For passenger car engines, which rarely have more than eight cylinders, the major part of the knock signatures from the successive cylinder events are not superimposed in time, but rather consecutive without overlap. The time delay due to the distance from the cylinder to the sensor is always much less than 1 ms, whereas the cylinder-to-cylinder time is 2.5 ms even for an eight-cylinder engine at 6000 rpm.

However, the *absolute amplitude* of the knock signal does vary from location to location on the block. There is no best place to mount the sensor; rather, a site with a strong amplitude should be selected for a given engine model, and the sensor should always be mounted at that point on that engine model. The knock threshold is experimentally determined on that engine model with the sensor mounted at that location.

The method used for processing the knock signal and effecting control was described in Sec. 8.2.4. As time has gone on, the knock signal processing has tended to become simpler, although in the 1990s this may be changing. Time windows and mechanically resonant sensors have largely disappeared, and much of the filtering is now done digitally.

8.3.2 Accelerometer Sensors

The magnetostrictive jerk sensor, while satisfactory in performance, has too many parts to be a low-cost solution to measuring knock on board. Moreover, its mechanical assembly is not simple. In an effort to achieve lower-cost solutions, the industry found that the second-time derivative of displacement—acceleration—could be measured and used to implement a satisfactory knock control. The drawback to using an accelerometer compared to a jerk sensor is that it does not yield as good a signal-to-noise ratio; however, by using appropriate filtering, a good control signal can be achieved.

The first accelerometers used were mechanically bandpass-tuned, and some still are. However, in the 1990s, the trend has been to broadband sensors, again used with much electronic filtering. This has the advantage that one sensor model can be used for all engines, with the engine-specific frequency filtering characteristics built into the electronics module, which has to be engine-specific anyway. If the crucial filtering features are provided digitally, they can be installed as part of the engine-specific software.

Piezoelectric Accelerometer. Certain crystals of a specific cut or orientation possess the property that, when stressed, they produce a corresponding voltage. If such a crystal is loaded with a mass and spring, vibrations entering the assembly squeeze and pull the crystal with respect to the mass, and result in a signal which is a measure of the acceleration of the body to

PETITIONER'S EXHIBIT 1002
US PATENT NO. 6,557,540

which the assembly is attached. These signals can be substantial in size but appear electrically to be sourced at a high (capacitive) driving point impedance. Thus, care has to be taken to ensure that capacitively coupled noise does not contaminate the signal.

There are a variety of single crystals which exhibit the piezoelectric effect, but silicon is not one of them. Efforts to devise a silicon micromachined accelerometer were stymied for a long time by this fact, but a solution will be described below. Single crystal quartz is the material which was used in the single-crystal piezoelectric accelerometers.

In some cases, it is possible to use the mass of the piezoelectric element itself as the mass, and to combine the spring with one of the crystal electrodes. In such a design, the only parts are a spring, a contact, the crystal, and the housing.

Piezoceramic Accelerometer. Another type of piezoelectric element is the piezoceramic device. Piezoceramics are not single crystals. They can be fired into just about any shape, just like a ceramic insulator or a vase. By impressing a high voltage across electrodes on the ceramic while the material is at a high temperature—above its Curie temperature—and then gradually lowering the temperature, the piezoceramic becomes *poled*, or piezoelectric across the electrodes.

The best piezoceramics tend to belong to the lead-zirconate-titanate (PZT) family. These materials have a Curie temperature from 250 to 500 °C. If the sensor ever gets above its Curie temperature, its poling becomes degraded, and its calibration is no longer valid. However, these engine block-mounted sensors will not experience temperatures higher than about 125 to 150 °C, even during hot soak, so they can be used for the knock sensor.

Single-crystal piezoelectric accelerometers also have a Curie temperature, but it is typically much higher than for the piezoceramics. Quartz, for example, has a Curie temperature over 600 °C.

Because the piezoceramic materials can be molded into any shape, handled roughly, sawn and machined, coated with thick-film metallic electrodes, and so on, they lend themselves to easy, low-cost mass production. As a result, they have become pretty much the knock sensor of choice for the automobile industry. A drawing of a piezoceramic accelerometer knock sensor is shown in Fig. 8.2. In this particular design, the spring and top electrode have been combined into one part, but the mass is a separate metallic part between the piezoceramic disc and the spring. The whole assembly is stacked on a mandrel which extends up from the base-stud which forms most of the package.

8.3.3 Silicon Accelerometer

As previously noted, silicon itself cannot be made piezoelectric. However, it is possible to make a silicon micromachined accelerometer by anisotropically machining a cantilevered T-shaped structure into each cell of a silicon wafer, using a chemical etch. Strain gauges are diffused or implanted into the cantilever—the vertical bar of the T. The mass of the horizontal crossbar of the T and the spring constant of the cantilever provide the mechanical-to-strain transduction. Such accelerometers are in mass production for use in antiskid braking systems and as triggers for air bag safety devices. Whether or not they will replace piezoceramic knock sensors is primarily a matter of economics. Technically, the silicon accelerometer is satisfactory; its temperature limit is about 150 °C, which is adequate for on-block mounting.

8.3.4 Other Sensors

Instantaneous Cylinder Pressure Sensor. The direct measurement of instantaneous cylinder pressure permits the extraction of the pressure reverberation signal, which is the direct cause of knock. While this would be a very desirable signal to use for knock detection, it has not been implemented in on-board knock control systems for several reasons:

PETITIONER'S EXHIBIT 1002
US PATENT NO. 6,557,540

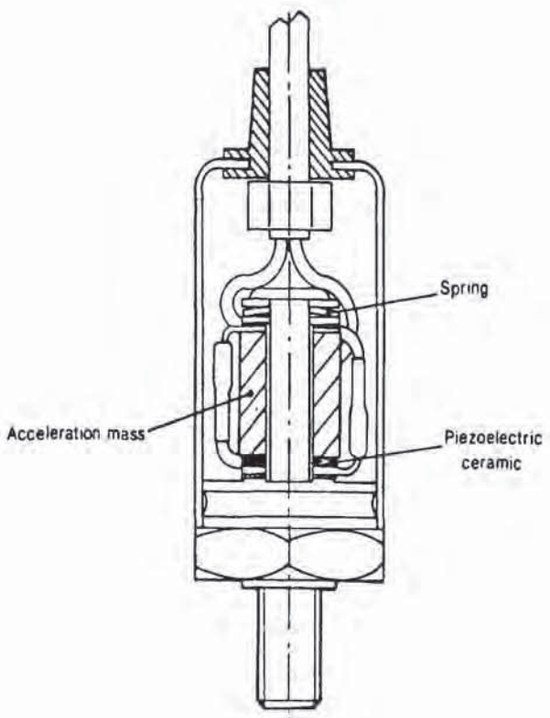


FIGURE 8.2 A piezoceramic accelerometer knock sensor.

- Either the same cylinder must always be the one to experience knock first and most severely, or one must have a sensor on every cylinder.
- The cylinder pressure wave is complex, and knock is only one of many signature elements present. Deriving a unique knock signal requires considerable signal processing in real time.
- While cylinder pressure sensors exist which are suitable for test purposes, a durable, low-cost, mass-producable on-board pressure sensor is not yet available.

In spite of these difficulties, work continues on cylinder pressure sensors for on-board control use, not so much to be used as knock-sensing devices as for use in deriving an instantaneous torque measurement (see Chap. 9). If this approach succeeds, then it is reasonable to suppose that the cylinder pressure sensor will be used to provide the inputs for obtaining both torque and knock measurements.

Since a spark-ignited engine already has a spark plug mounted in each cylinder head, it is possible to convert the spark plug into a kind of "poor man's pressure sensor" by mounting a piezoceramic washer held in compression between the spark plug and the cylinder head when the plug is torqued down. This arrangement has in fact appeared on a commercial passenger car engine. While the signal is not presently being used to extract a knock signal, suitable signal processing would make this possible.

Hydrophone in Coolant. In Sec. 8.3.1, it was mentioned that the knock signal appears virtually everywhere on the block. In fact, it even appears in the coolant fluid faithfully reproduced. This fact led to experiments in which hydrophones were mounted in the coolant and used as knock sensors. This approach has never reached production because it has no advantage over a block-mounted sensor and is in fact more difficult to package and to mount on the engine.

PETITIONER'S EXHIBIT 1002
US PATENT NO. 6,557,540

8.4 SUMMARY

In a remarkably short span of time, the on-board sensing of knock and its control have become a rather standard feature of passenger car engine control electronics. At the same time, the on-board sensors have been developed and are now largely mature. Acceleration has become the parameter of choice for most of these control systems, and the required accelerometers are typically based upon piezoceramic technology; it seems likely that this will remain the case at least through the 1990s. The rapid proliferation of these systems was facilitated by three factors:

- A solid background of experimental knowledge about knock and how to control it was established in the laboratory during the several decades before lead-free gas was mandated.
- The three legislated pressures of emissions limits, CAFE fuel economy goals, and no-lead fuel, combined with a customer base used to engines without knock, made solving the knock problem a high priority.
- The already widespread use of digital microcomputer engine control made the addition of knock limit control a straightforward design change.

GLOSSARY

Curie temperature The temperature above which a piezoelectric crystal or piezoceramic element no longer reliably retains its original piezoelectric characteristics.

Jerk sensor A sensor which measures the third-time derivative of displacement.

Knock Acoustic engine noise and vibration of characteristic frequency caused by uneven combustion in the engine cylinder(s).

Octane rating A measure of the resistance of a gasoline fuel to knock, as compared to pure isooctane hydrocarbon.

Retarding Causing engine combustion to occur at a larger angle past top dead center, by delaying the time at which the signal to start the spark event occurs.

Turbocharger A device which compresses engine intake manifold air by using the engine exhaust to drive a turbine and compressor.

Wastegate valve A valve in the exhaust system of a turbocharged diesel engine which causes part of the exhaust to bypass the turbine. The same name is also applied to a valve on a turbocharged gasoline engine which causes part of the boosted intake manifold air to dump to the atmosphere, dropping the manifold pressure.

REFERENCES

1. Paulius V. Puzinauskas, "Examination of methods used to characterize knock," SAE Paper 920808, Superflor Corp.
2. Karp P. Schmillen (FEV Motorentechnik, Aachen, Germany) and Manfred Rechs (Institute for Applied Thermodynamics, Technical University of Aachen, Germany), "Different methods of knock detection and knock control," SAE Paper 910858.
3. Masayoshi Kaneyasu (Hitachi America, Ltd.), Nobuo Kurihara, Kozo Katogi, and Hiroatsu Tokuda (Hitachi Ltd.), "Engine knock detection using multi-spectrum method," SAE Paper 920702.

ENGR & MATH SCI LIBRARY UMC

PETITIONER'S EXHIBIT 1002
US PATENT NO. 6,557,540

ABOUT THE AUTHOR

William G. Wolber, executive engineer, Cummins Electronics Co., Inc., has 38 years' experience in the development of sensors, actuators, and instruments for application in automobiles and other products. Since 1981, he has been involved principally in the development of sensors and controls for heavy duty diesel engines for Cummins Electronics Co. He holds 15 U.S. patents and is the author of over 50 technical papers. He has lectured and conducted seminars internationally for the Society of Automotive Engineers and other organizations.

PETITIONER'S EXHIBIT 1002
US PATENT NO. 6,557,540

CHAPTER 9
ENGINE TORQUE SENSORS

William G. Wolber
Executive Engineer
Cummins Electronics Co. Inc.

9.1 INTRODUCTION

Torque is one of the primary state parameters of an engine; along with speed it is a fundamental measure related to the output power. Torque can be defined as the moment produced by the engine crankshaft tending to cause the output driveline to turn and thereby deliver power to the load. For rotary motion, the torque multiplied by the rotational speed equals the power delivered by the shaft. In derivative form, Newton's law states that torque T equals the rotational moment of inertia I times the angular acceleration α. Hence, at constant rotational speed, instantaneous power is proportional to instantaneous torque. This is an important relationship because torque and, thus, delivered power can change rapidly compared to rotational speed.

Portraying the engine as a torque-delivering device is a useful concept. When an engine is used in road service as prime mover power, the operator of the vehicle tends to ask the vehicle for positive or negative incremental acceleration, as the operator perceives it to be falling behind or closing upon the vehicle ahead. Hence, the operator asks the engine for more or less torque. If the engine is spark ignited, this happens naturally through the modulation of the engine air intake flow path. In a diesel engine, it happens indirectly. The operator controls fuel rate, which to first approximation is linearly related to power. For slowly varying engine speed and load, an incremental change in power results in a change in torque and therefore a change in acceleration.

9.1.1 Time-Scale Definitions

At this point, it is useful to define two time scales which will be used with regard to the engine. A reciprocating engine is never truly operating steady state. It is a cyclic succession of batch processes, a kind of system which chemical engineers have termed "continuous-by-jerks." Each cylinder absorbs shaft energy during the compression stroke and releases a larger amount of shaft energy through combustion during the power stroke. These actions are so interleaved that the drive shaft is continually accelerating and decelerating in step with cylinder events. Nevertheless, a quasi-steady-state model for the engine can be defined in which these rapid fluctuations are ignored and attention is focused on the more slowly varying state parameters which are nearly stationary during one engine revolution. This is the situation the operator senses and controls and it is also the primary focus of the control algorithms in a microcomputer-based engine control today. (As of 1994, all electronic engine controls operate on the "engine time scale.")

PETITIONER'S EXHIBIT 1002
US PATENT NO. 6,557,540

Quasi-Steady-State Torque. Quasi-steady-state torque is defined as that running average value of torque that varies slowly with respect to the cylinder-to-cylinder period, but rapidly with respect to vehicle changes in motion and load. To quantize this state, it is noted that an unloaded engine coupled to flywheel inertia may accelerate from idle to maximum speed in one to five seconds when subjected to wide open throttle and that this performance is essentially reproduced whether the change in throttle position occurs in 20 ms or 1 ms. Quasi-steady-state torque is what the operator is interested in commanding, and so, if we visualize a torque command-feedback engine control, it is the parameter of interest.

Instantaneous Torque. Today's electronic engine control can usefully respond much more rapidly than this for those state parameters having to do with each cylinder batch process itself. The preparation of the fuel and air charges and the timing of ignition take place on a time scale measured in fractions of a cylinder period, and thus the time scale of interest ranges from 30 μs to 20 ms. This time scale corresponds to the instantaneous engine state. It is the time scale of the torque impulses that are termed instantaneous torque.

In order to use instantaneous torque measurements, it must be recognized that the reciprocating engine is a cyclic machine in which major functions and the parameters that characterize them are tied together in sequence mechanically by the crankshaft and camshaft. Proper adjustment of those other parameters that are free to be changed independently of the train of instantaneous cylinder events allows optimization of the overall torque impulse generation in real time. For example, a theoretical examination of the internal combustion engine cycle has shown that the centroid of the cylinder pressure wave should occur about 15 crank-angle degrees after top dead center ("Powell's Magic Angle") to maximize the instantaneous incremental torque from that cylinder.[1,2] No spark or injection timing algorithm can do any better than to effect such timing of the torque impulse. Note, however, that we are stating where the centroid of the pressure wave should be for the best torque impulse, not where the fuel injection or ignition should be commanded.

State-of-the-art scheduled spark timing controls are based upon test data from one or more prototype engines run extensively in the laboratory on a dynamometer under quasi-steady-state conditions. From the data obtained, families of spark plug or injection timing (crank angle) surfaces versus engine speed, load, etc., are derived that correspond to optimum economy and performance while meeting emission requirements. These data then form the schedule embedded in the control microcomputer memory for all engines of that model produced. This type of scheduled computer control is standard throughout the industry today for all electronically controlled engines, both spark-ignited and compression ignition, with just two exceptions. These are the oxygen sensor feedback control loop, which keeps an engine equipped with a three-way catalyst in the stoichiometric "window" of the catalyst efficiency performance, and the speed governing feedback control algorithm used for power takeoff (PTO) operations, diesel all-speed governors, and generator-set frequency control.

By contrast, the addition of an on-board instantaneous torque measurement would permit the direct feedback control of several key engine control parameters. To take maximum advantage of such feedback control, an advanced instantaneous crankshaft position sensor is also required.

The controls which could be implemented through use of an instantaneous torque feedback control system are:

- Quasi-steady-state torque feedback control in response to torque command.
- Spark-ignition or compression-ignition timing control by feedback of instantaneous torque impulse timing compared to the norm of the "Magic Angle." Torque impulse amplitude can also be optimized against timing. These controls can be implemented on a cylinder-by-cylinder basis, for spark-ignited pulse sequential fuel injected engines, and for unit-injected diesel engines.
- Cylinder-by-cylinder torque-leveling feedback control can be implemented by adjusting the amount of fuel injected into each cylinder to obtain equal torque impulses from each one.

PETITIONER'S EXHIBIT 1002
US PATENT NO. 6,557,540

This results in a quiet, smoothly running engine with a somewhat improved maximum power, because the torque limit can be set for a more nearly constant cylinder event instead of for the worst case cylinder.

- The instantaneous torque signal is also rich in a variety of diagnostic information—for example, to measure engine power or for use as a miss detector.

9.2 AUTOMOTIVE APPLICATIONS OF TORQUE MEASUREMENT

9.2.1 Off-Board Measurement

The principal automotive use of torque measurement today is in the testing and evaluation of engines using the engine dynamometer. The torque sensor is inserted as a drive shaft between the engine and the dynamometer; the shaft of the sensor is a torsional Hooke's law member and its twist is measured. Typically the torque is actually measured using a strain gage bridge on the drive shaft. Full-scale twist is limited to no more than about a degree per foot of shaft for engines in the 50 to 500 hp range.

In a dc torque sensor, the strain gage bridge is powered from an external source through slip rings, and the offset voltage is taken off the bridge the same way (Fig. 9.1). The sensor is necessarily bulky, large, fragile, and costly. A more rugged ac strain gage sensor can be made using rotational transformers, as shown schematically in Fig. 9.2.

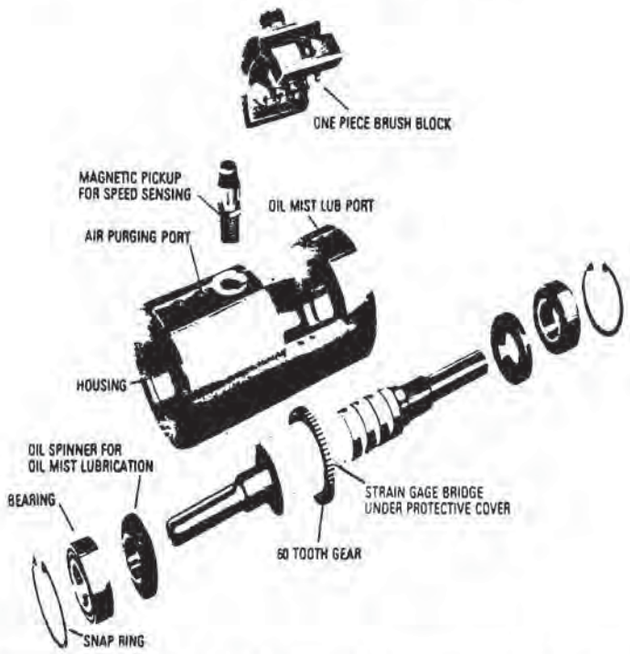


FIGURE 9.1 Exploded view of rotating shaft torque sensor with slip rings. *(Courtesy of the Lebow Div., the Eaton Corp.)*

Developmental Tests. In engine development, a good bit of the work involves fine-tuning the engine to get the maximum power and minimum fuel consumption at various engine conditions. Since power equals torque multiplied by engine speed, if tests are carried out at constant speed, maximum power occurs at maximum torque. Thus, the torque sensor can be used as a direct indicator of whether changes in the engine design or control will improve power.

PETITIONER'S EXHIBIT 1002
US PATENT NO. 6,557,540

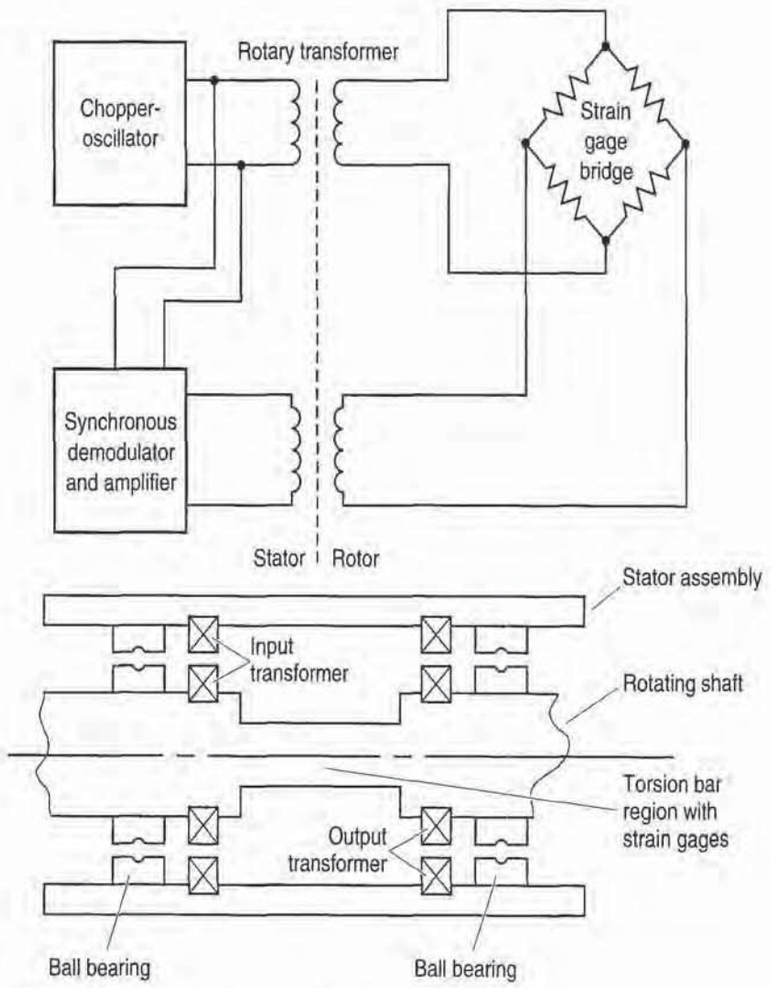


FIGURE 9.2 Rotary transformer rotating shaft torque sensor.

End-of-Line Manufacturing Tests. Particularly in the case of heavy duty diesel engines, the price of the engine is directly related to engine rated horsepower. Such engines are in a real sense sold by the horsepower. The manufacturer certifies that a certain model will deliver no less than a certain horsepower when run at rated conditions. The engine is tested at the end of the assembly line for a number of attributes, chief among which is assurance that it exceeds stated horsepower at rated speed. The assurance is provided by accurate torque and speed measurements.

In-Service Tests. Occasionally, torque sensors may be used with an engine that is being tested under field conditions. This is relatively straightforward when the engine is being used in a stationary application, but not if it is installed in a vehicle.

9.2.2 On-Board Measurements

To be most useful on board, a torque sensor should not only be accurate but also fast in response. Most of the sensors available today do not have this attribute, because they were developed for use in dynamometer tests.

To be a useful on-board engine control sensor, the torque sensor of the future also needs several other attributes:

PETITIONER'S EXHIBIT 1002
US PATENT NO. 6,557,540

- It must be extremely rugged, which for practical purposes means noncontacting with respect to the driveline.
- It must be able to withstand torque impulses of 10 to 20 times its full-scale measuring capability without degrading its accuracy. For strain gage type sensors, this means that the sensor would always have to measure in the lowest 5 to 10 percent of its range, where it is not very accurate.
- Installation of the sensor must not cause any significant change in the compliance of the driveline. This is a requirement imposed by engine application engineers to avoid spoiling the tradeoffs that have been made to avoid severe torsional vibrations.
- Ideally, the shaft of the sensor should be very short in length (in part to achieve the preceding characteristics). Unfortunately, for a torsional Hooke's law device, that means the full-scale shaft twist angle will be very small.

In spite of these formidable barriers to a satisfactory design, a wide variety of desirable applications could be made using an on-board instantaneous torque sensor. As a result, many researchers and developers both in academia and industry are working to achieve such a measurement directly or indirectly.

Power Measurement of Large Engines. Means exist for field service personnel to measure engine power in the field for engines installed in a vehicle and rated at up to 400 to 500 hp. For larger vehicle-mounted engines, this measurement is a difficult problem for a number of reasons:

- A rugged on-board sensor is not available.
- These engines are often installed in very large machines such as mine-haul trucks and front-end loaders located off the road in remote areas.
- Dynamometers large enough to load down the engine to full power are not available except in a very few locations.

One of the most frequent customer complaints about heavy duty engines is perceived loss of power. Often such complaints must be resolved at the field location and on a subjective basis. The engine and vehicle can be fully loaded in actual work operation, and engine speed is known accurately. If an on-board torque sensor were available, such complaints could be quickly resolved, and it would be well worth installing on large engines.

Miss Detection. The California Air Resources Board has mandated that all passenger vehicles shall be equipped with an engine diagnostic capability that includes a miss detector. While the regulation is not yet in force as of the time of this writing, the automotive industry knows that every segment will be affected by the requirement by the end of the decade. Many vehicle OEMs, first-tier automotive suppliers, entrepreneurial sensor firms, and academic researchers are working hard to meet the miss detector requirements, mainly basing their efforts on the same technologies useful for measuring or inferring torque.[3]

Torque Feedback Control. The reciprocating engine could be configured in a feedback control mode if equipped with an on-board quasi-steady-state torque sensor capable of responding at least as fast as the engine/driveline. In a torque command drive-by-wire system, the operator input would be a command for a new torque, greater or less than the present torque. The engine control would do its best to provide the new torque as rapidly as possible. The feedback error signal would be the difference between the torque command and the sensor output. Of course, the new torque and the resulting acceleration or deceleration would have to be limited within bounds set by maxima for cylinder pressure, emissions production, exhaust gas temperature, fuel economy, and so on.

Feedback Control of Timing. As was described in the introduction to this chapter, the measurement of instantaneous torque, on board, along with instantaneous crank angle position,

PETITIONER'S EXHIBIT 1002
US PATENT NO. 6,557,540

would allow the engine control computer to use signature recognition to measure the crank angle at which the centroid of the torque impulse is located, for each cylinder. From this information, probably with some compensation for seriously off-normal engine conditions as stored in computer memory, the engine control can determine if that impulse was centered at Powell's Magic Angle, and, if not, how much earlier or later the chain of combustion events needs to be started. Most likely, the computer also needs to decide between updating that cylinder based upon that information alone and waiting a whole engine revolution to update, or also basing the correction upon abrupt changes in operator input, load, knock level, etc. In any case, under quasi-steady-state conditions, the best efficiency of that engine for converting chemical energy into shaft power by proper engine timing could be achieved this way whether the engine is spark-ignited or compression-ignition.

Cylinder Torque Leveling. Individual trimming of the amount of fuel for each cylinder can be realized on pulse sequential fuel injected spark-ignited engines and on unit injector diesel engines by matching the torque impulse for each cylinder to the average of all cylinders. Then the average impulse can be raised to very nearly the maximum value the engine is designed for. In today's engines, the control must provide a guard band between the maximum torque for the worst case cylinder and the design limit for the engine (commonly called the maximum cylinder pressure limit or the peak torque limit). If the torque impulses delivered by each cylinder were known to be controlled to be equal, the guard band could be reduced and more power obtained from a given engine.

While cylinder-to-cylinder torque leveling is not the same as compression leveling, an engine controlled cylinder by cylinder for timing and torque leveling intuitively would appear to be as smoothly running and low in acoustic noise emission as can be visualized.

Engine Diagnostics. The instantaneous torque signature is very rich in diagnostic information. A figure of merit for engine roughness can easily be obtained in real time, from which a lean-limit control signal can be derived. The miss detector responds to an extreme case of roughness. Ragged ignition and flame front formation, imperfect injection, poor distribution, and many other engine and control problems can be measured or inferred from such a signal, on board and in real time.

9.3 DIRECT TORQUE SENSORS

9.3.1 Reaction Force

The use of a strain-gaged torsional Hooke's law shaft to measure torque at the dynamometer has been described in Sec. 9.2.1. Torque can also be measured in the test cell by instrumenting the engine or dynamometer mounting with strain gage load cells to measure reaction torque. This is a useful way to measure quasi-steady-state torque, but is not a good measuring system for instantaneous torque, as both the engine and its load have considerable inertia and damping which attenuate the torque impulse and may introduce phase delay. It is also not a good on-board measurement because the engine mounts on a vehicle are designed to attenuate and damp out bouncing from road and load irregularities. Also, as a function of time, temperature, ozone concentration, and other variables, they tend to stiffen substantially and change the deflection of the engine at its mounts as a function of torque.

9.3.2 Torsional Strain (Twist) Sensors

Magnetic Vector Sensors. The strain-gaged torsional Hooke's law sensor was described in Sec. 9.2.1. A more practical approach to an on-board torque sensor is a noncontacting design

PETITIONER'S EXHIBIT 1002
US PATENT NO. 6,557,540

called a magnetic vector sensor.[4,5] This sensor operates on the principle that the magnetic domains in a ferromagnetic shaft delivering torque are randomly distributed when no torque is being delivered, but that each domain, on average, is slightly rotated in the tangential direction when torque is delivered by the shaft and twists it. If an ac-driven coil is placed near the shaft and surrounded by four sensing coils arranged mechanically and electrically as a bridge, the amplitude of the bridge offset is proportional to the magnetic vector tangential component, and therefore to twist and torque.

If the magnetic domains were truly statistically distributed over a small range of shaft angle, such a sensor would be able to measure instantaneous torque. Unfortunately, they are not. Over a small shaft angle increment, the average torque vector does not net to zero when torque is zero, and the output is characterized by a fixed pattern noise which repeats every 360°. The magnetic vector sensor is reasonably accurate measuring quasi-steady-state torque, but the signal-to-noise ratio becomes poor when an attempt is made to measure instantaneous torque.

Further work on this sensor simplified and miniaturized it.[6] The bridge was replaced by a single tangential coil, and the sensor was made small enough so that it could be mounted in the rear crankshaft bearing. However, it still was not able to measure instantaneous torque.

Investigation continues on techniques to reduce the fixed pattern noise, and some claims of progress have been made. However, at this writing, a production on-board torque sensor is not available.

Optical Twist Measurement. Research work has been reported on a sensor that changes the duty factor of light pulses sensed after passing through sets of slits at both ends of a shaft.[7] The principle of its operation is shown in Fig. 9.3. Such a sensor is noncontacting and can be made robust, but it requires appreciable shaft length and therefore adds compliance to the driveline. The work has not been engineered to produce an economical on-board device.

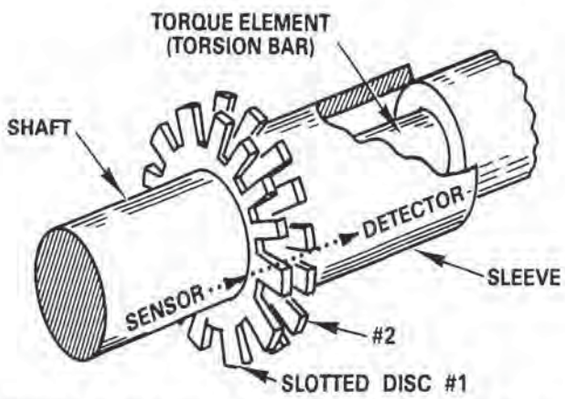


FIGURE 9.3 Optical torque meter. *(Courtesy of The Bendix Corp.)*

Capacitive Twist Sensor. An electrode pattern can be made using interdigitated electrodes spaced one or two degrees apart on two facing flat discs.[8] One of the discs is stationary; the other rotates with the crankshaft. Two such pairs of electrodes can be operated with phase detection measurement to provide a virtually instantaneous signal proportional to the twist of the shaft; the rotating halves of the electrode pairs are attached to the ends of the Hooke's law torsional spring. Obviously, this arrangement has the same drawback as the optical sensor in that it has to have some shaft length to twist and, therefore, some compliance. However, it is robust, has good accuracy, and is a more practical on-board device than the optical twist sen-

ENGR & MATH SCI LIBRARY

PETITIONER'S EXHIBIT 1002
US PATENT NO. 6,557,540

sor. This sensor can also yield an accurate crankshaft position measurement. Nevertheless, an on-board version is not available today.

9.4 INFERRED TORQUE MEASUREMENT

Indirect measurements of torque-related parameters can be made with a view to inferring torque from the measurements. Typically, such measurements require considerable real-time computation in the control microcomputer, along with precision measurement of the instantaneous crank angle position. Much work is in progress in a variety of locations to make these methods into practical instantaneous torque control signals.

9.4.1 Instantaneous Cylinder Pressure Sensors

Engine development engineers have long used piezoelectric crystal cylinder pressure sensors in the laboratory to make engine power and heat release measurements and as an aid to development. The best of these sensors use doped quartz single crystals. They are accurate and reasonably robust, but expensive and unforgiving if overranged or subjected to excessive temperatures. Much work continues on development of a mass-producable on-board cylinder pressure sensor.[9] One of the Japanese car manufacturers is reported to have a top-of-the-line passenger car model, available only in Japan, with engine control using piezoceramic cylinder pressure sensors.

The signals from cylinder pressure sensors need considerable real-time data processing to produce inferred "torque" signals. In one method, the noise always present is filtered, the pressure signal is multiplied by an instantaneous shaft angle term, and integrated over the angle range representative of the power stroke of the cylinder. From this a measure of torque contribution from that cylinder is obtained. The best digital signal processing (DSP) chips available in the early 1990s are barely able to keep up with cylinder events in such a process. Nevertheless, we can be confident that if the proper sensors are available in the late 90s, the microcomputer chip performance required will be available and cost effective too.

9.4.2 Digital Period Analysis (DPA)

When an engine is run at low speed and heavy load, the instantaneous angular velocity of its output shaft on the engine side of the flywheel varies at the fundamental frequency of the cylinders, since the compression stroke of each cylinder abstracts torque and the power stroke adds a larger amount. The signal-to-noise ratio of the measurement of instantaneous angular velocity (or rather of its reciprocal, instantaneous period) degrades with increasing engine speed and lighter load, but is a useful way to infer torque-like measures of engine performance.

Figure 9.4 shows an idealized plot of instantaneous crankshaft period against crank angle under constant speed, lean conditions. The instantaneous period wave is seen to be a variation about the mean period value. This waveform can actually be measured using a precision, multitoothed crankshaft position sensor. For reasons which will be explained later, the instantaneous angular velocity lags the torque inputs producing it. As a result, the period wave appears to lead the torque or cylinder pressure variations.

Timing Control by DPA. The general case of the variation in crankshaft velocity in a four-cylinder engine can be described by:

$$T_N = AL\,P_N(\theta)\sin\theta = AL\,P_{(N+3)}(\theta)\sin\theta + T_F(\theta) + T_L + I\ddot{\theta} \qquad (9.1)$$

PETITIONER'S EXHIBIT 1002
US PATENT NO. 6,557,540

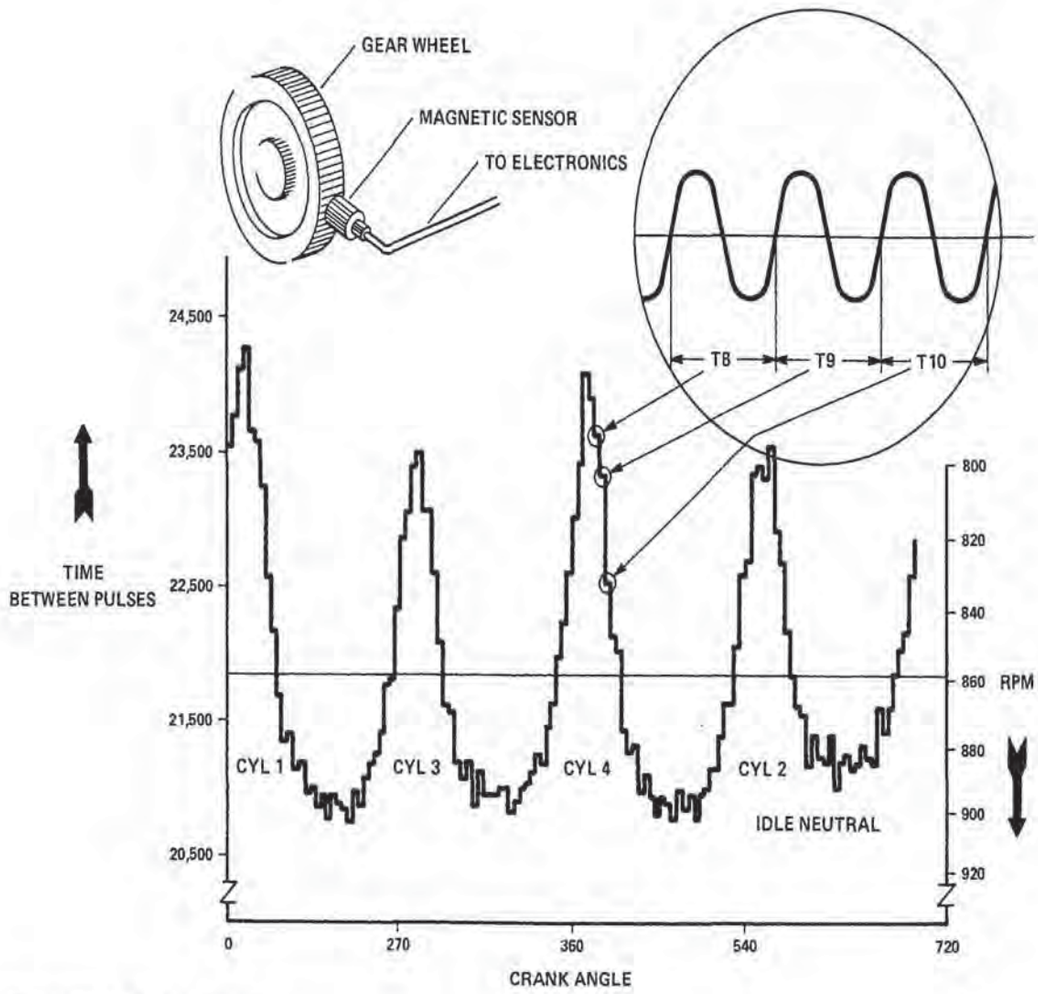


FIGURE 9.4 Digital period input.

where T_N = instantaneous torque due to burning gases in cylinder N at angle θ
A = area of piston
L = maximum effective crank lever arm
$P_N(\theta)$ = pressure in cylinder N (a function of crank angle and many other variables)
$P_{(N+3)}(\theta)$ = pressure in third cylinder to fire after N which is in its compression stroke when cylinder N is in its power stroke
$T_F(\theta)$ = so-called "fixed load" torque due to friction, accessories, etc., and is generally a function of $d\theta/dt$
T_L = torque delivered to the load
I = inertia of the engine, drivetrain, and vehicle reaction through the wheels
$\ddot{\theta}$ = instantaneous angular acceleration of the crankshaft

In order for Eq. (9.1) to remain valid, as T_N varies with angle θ due to the variations of $P_N(\theta)$ and the sin θ term, some term in the right-hand side of the equation must vary correspondingly. In fact, the major effect is upon $\ddot{\theta}$, the angular acceleration, which varies both in magnitude and sign; being positive when P_N is large and θ is near $\pi/2$, and negative when P_N is small and θ is near 0 and π. If Eq. (9.1) is integrated as a function of θ from $\theta = 0$ to $\theta = \pi$ and

PETITIONER'S EXHIBIT 1002
US PATENT NO. 6,557,540

then the summation is extended to angles larger than π by adding in the contributions of cylinders $N + 1$ and $N + 3$, the term in $I\ddot{\theta}$ becomes an average angular velocity over a complete engine cycle.

One important consequence of the preceding analysis is that, upon integration of the equation, the sin θ term becomes cos θ—that is, the angular velocity wave lags the torque impulses causing it by π/2. Another consequence is that the amplitude of the period wave reflects the net contribution of the cylinders—if the load increases, and $P_N(\theta)$ increases to keep average angular velocity constant, the amplitude of the period wave must increase. The $I\ddot{\theta}$ term has become an $I\omega$, it is the reciprocal of this term which was plotted in Fig. 9.4.

When a spark plug fires or fuel is injected into a diesel cylinder, the pressure in the cylinder takes a finite length of time to build—first, because of a delay to get the fire started and then because of the finite and relatively constant flame propagation time, and second, because the temperature rise which causes pressure to rise, peaks only shortly before combustion is completed. Thereafter, pressure falls as the piston displaces under the pressure of the gases. Mean best torque (MBT) will be achieved from that cylinder when the pressure pulse, convolved with sin θ yields a maximum upon integration. As described previously, researchers at Stanford University have found analytically and confirmed experimentally that this condition prevails for a fairly wide range of engine conditions when the centroid of the pressure pulse occurs at 15 degrees past top dead center (TDC). Because of the delays described previously, ignition must occur early enough to position the pressure peak near this value. It is this "anticipation" in spark plug firing that is termed *ignition advance*. The reason why advance angle has to be larger at higher speeds is now obvious: the flame propagation delay time covers more degrees of crank angle when the engine is running faster.

Further experiments by the Stanford researchers and others confirmed the suspicion that the period wave is a strong function of the crank angle, and that the angle associated with the centroid of the pressure wave is a unique function of the phase of the fundamental component of the period wave measured with respect to a crankshaft angle index point, say top dead center of cylinder no. 1. The period wave is measured with a sensor which is a precision version of a crankshaft position sensor.[10] It produces a fast, sharp pulse for every small and equal angle increment—say one degree—through which the shaft turns. Pulses from a high-frequency quartz crystal clock are counted to measure each period. The crankshaft angle index is available from the crankshaft position sensor. In principle, the period wave could be Fourier analyzed into the Fourier integral coefficients A_n and B_n by computing the Fourier integrals, and the phase of the fundamental (first harmonic) is then arctan B_1/A_1. To perform this computation in real time is a bit much to ask of today's microcomputer (but not tomorrow's!) and various shortcuts are utilized to achieve an approximate result. Remembering that the period wave appears to lead the torque impulses that cause it by π/2, the spark timing can now be varied so as to place the centroid of the pressure wave, on the average, at or very near the 15-degree-after-TDC point.

It is instructive to consider what performance is required of the DPA and crankshaft position sensors to achieve a given signal-to-noise ratio. The repeatability of the crankshaft angle marked by the sensor is a function of the diameter of the sensing disc. For the various magnetic sensors, a repeatability better than ±0.5 degree can be achieved with a 10-cm-diameter disc. In the DPA sensor, the concern is for the period-to-period jitter. It is obviously worse for smaller angle increments both because the angle jitter is a larger part of the period, and also because the period-counting roundoff error is larger for any given clock frequency. At the same time, the more periods measured per revolution, the more fidelity the period wave will have for its high-frequency components. The period-to-period jitter of the magnetic sensor in this example is about ±0.5 degree. This is satisfactory for 24 periods per revolution but marginal for 60 periods; a typical period wave amplitude is only ±3 percent of the average period. On the other hand, even 60 periods per revolution is marginal for ignition or injection timing control.

The granularity due to counting roundoff also needs to be considered. Today's low-cost LSI circuits can count reliably at 20 MHz, so that is a practical clock frequency. If a four-cylin-

PETITIONER'S EXHIBIT 1002
US PATENT NO. 6,557,540

der engine is running at 1800 rev/min (30 Hz), the associated period wave will have a fundamental of 60 Hz. If the DPA sensor has one degree angle indices, referred to the crankshaft, each period will have about 2000 counts from the clock. Therefore, the period counting round-off noise will be ±1 part per 2000. Referred to a nominal ±3 percent amplitude period wave, this jitter amounts to ±2 percent of the peak value of the period wave (not of the period itself), not counting any smoothing.

For the fundamental of the period wave, the phase of which is used for DPA timing control, a good deal of smoothing can be realized, so that for a "clean" engine, estimation of the correct angle to ± one crankshaft degree is feasible.

Figure 9.5 shows an actual period wave measured using an electromagnetic DPA sensor with one-degree increments and a 10-MHz clock. Both the jitter described previously and a fixed pattern noise can be discerned in the signal. The latter effect is due to slight imperfections in the tooth spacing of the precision gear used as the sensing disc. Such systematic errors can be eliminated in the microcomputer, but they are troublesome and consume integration time. The better solution is to design a precision DPA sensor which minimizes fixed pattern noise.

DPA Used for Diagnostics. During the 1980s, one of the heavy duty diesel engine manufacturers introduced an off-board diagnostic instrument capable of doing DPA on the engine with the clutch disengaged and using snap acceleration and deceleration to load the engine

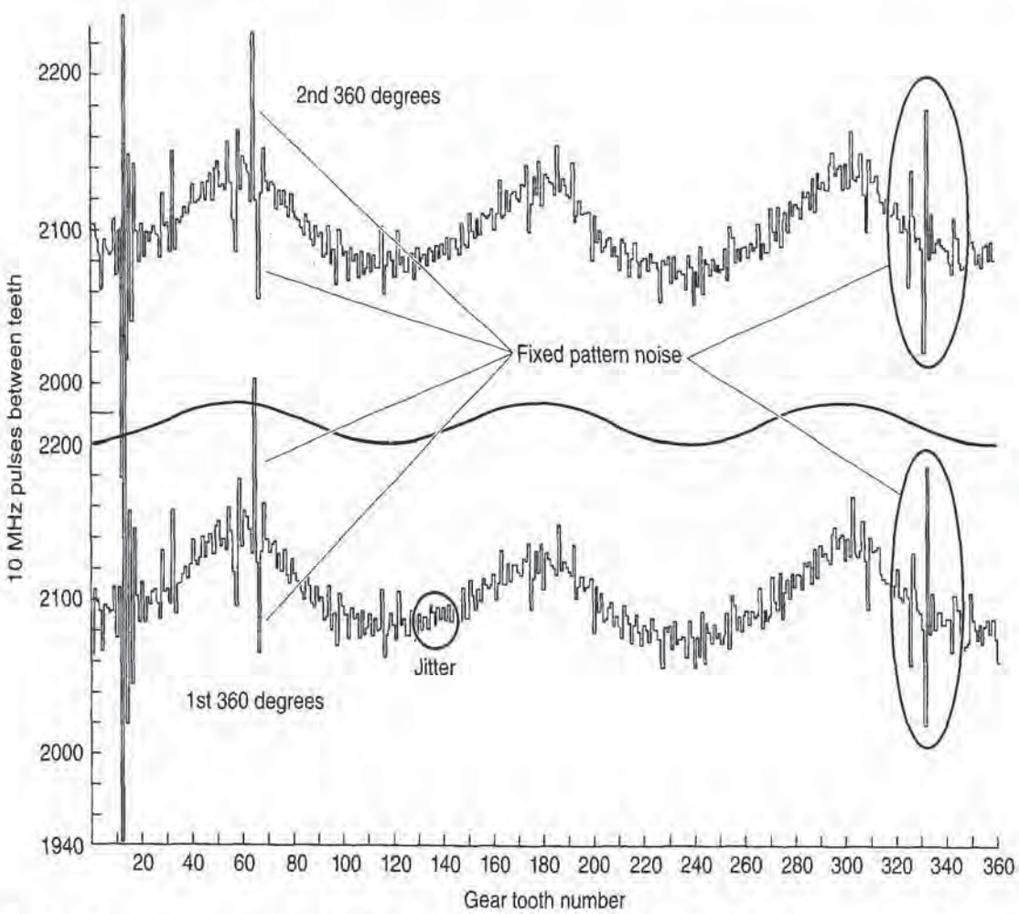


FIGURE 9.5 Actual period wave data from engine crankshaft; unsmoothed data. *(Courtesy of The Bendix Corp., Diesel Operation)*

ENGR & MATH SCI LIBRARY UCLA

PETITIONER'S EXHIBIT 1002
US PATENT NO. 6,557,540

inertially. This instrument used the very imperfect engine ring gear as the DPA target but solved the fixed pattern noise problem in a very elegant way.[11] The position sensor is actually a dual sensor, with the two magnetic circuits disposed tangential to the ring gear and closer together than one tooth pitch. A particular tooth is sensed by the first magnetic circuit and then by the second before the next tooth is sensed by the first circuit. Virtually all of the fixed pattern noise is eliminated.

What would be achieved in an on-board DPA system would be real-time, nearly ideal closed-loop control of spark timing. As with most controls for spark-ignited engines, there are some trims required to make the system work. Flame front propagation is in fact a complex process which has a substantial jitter in the time of propagation, so it is necessary to average the computation of the phase angle over a number of cylinder pulses in order to obtain a good phase estimator. Under transient conditions, the shape of the pressure pulse may change enough so that the angle for mean best torque (MBT) shifts slightly. These factors can also be incorporated in the control. A similar method could be used for compression-ignition engines; in fact, the period wave has a more reproducible signature than for a spark-ignited engine.

It is useful at this point to emphasize again that these principles hold under any conditions, but that the control works well only in the lean regime. As the air/fuel ratio nears stoichiometry, the amplitude of the period wave becomes quite small. Because the method of measuring the instantaneous period—counting clock pulses over a finite angle increment—is a differencing method, the signal-to-noise ratio (S/N) is always a problem, since a differencing process always yields a poorer S/N than that of the original function. Hence, the DPA technique yields poorer results the nearer the engine is to stoichiometry and the higher the engine speed.

Referring to Fig. 9.6, if a figure of merit is formed

$$R = \left| \frac{T_2 - T_1}{t_1 + t_2} \right| \tag{9.2}$$

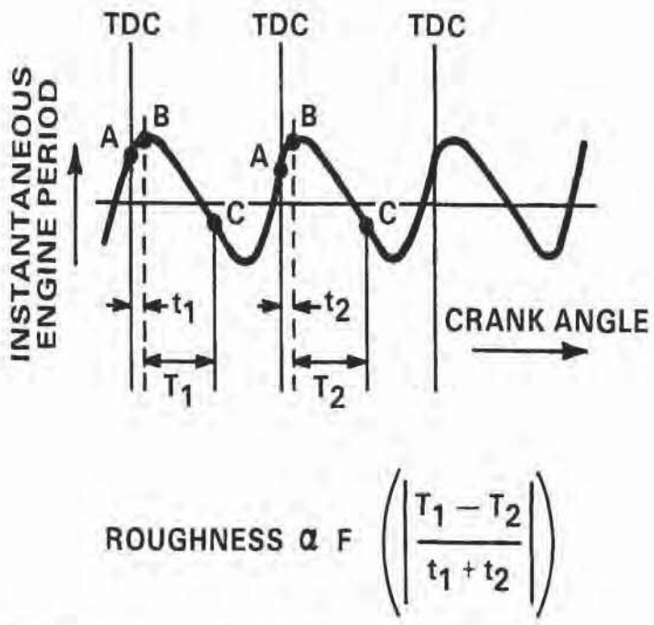


FIGURE 9.6 Digital roughness control.

PETITIONER'S EXHIBIT 1002
US PATENT NO. 6,557,540

we have a measure of the "roughness" of the engine useful for lean limit control or misfire detection. This is one example of many such optimizing algorithms which may be derived from DPA

9.5 SUMMARY

One can conclude from this chapter that torque measurement, whether direct or inferred, is a useful parameter for engine evaluation off-board, but that the proper sensors and computer analysis equipment for on-board control are not yet available. Yet the number of facilities working to advance this art, the resources being added, and the sporadic reports of progress are such that one can predict with some confidence that a breakthrough is imminent. Just what kind of control will first appear, and what kind or kinds will ultimately be successful, is not yet clear.

GLOSSARY

Algorithm A set of software instructions causing a digital computer to go through a prescribed routine. Because embedded computer engine controls have become so common, algorithm has become essentially synonymous with control law for automotive engineers.
Compression leveling A (theoretical) type of engine control which would cause each piston in each cylinder to compress its air charge to the same maximum pressure.
Dynamometer A machine to absorb power in a controlled manner, especially from an engine under test.
Hooke's law A relationship for an ideal elastic member which says that the displacement is proportional to the force.
Interdigitated An arrangement of two multiple-finger structures such that each pair of fingers from one structure has a finger from the other interposed.
Pulse sequential A type of fuel control for gasoline spark-ignited engines in which the fuel for each cylinder is injected into the air manifold near the intake valve for that cylinder just as it opens.
Robust Able to survive and operate properly in a severe environment.
Stoichiometric Pertaining to a combustion process in which the oxidizing agent (oxygen) and the reducing agent (fuel) are in balance such that, were the reaction to go to completion, there would be neither oxygen nor fuel left over, and all the reaction products such as carbon monoxide would be oxidized to their highest state—carbon dioxide.
Torsional Hooke's law A relationship for an ideal elastic shaft which says that the angle through which the shaft twists is proportional to the torque.
Torque The moment tending to make the output shaft of an engine turn. Torque can be expressed as a force acting perpendicular to a lever arm at a distance from the center of rotation. Its units are Newton-meters (pound force-feet).
Unit injector A type of fuel control for diesel engines which has fuel metered into a piston-barrel injector for injection into a specific cylinder at a specific time. Each engine cylinder has its own cam-driven injector, which operates something like a hypodermic syringe.

PETITIONER'S EXHIBIT 1002
US PATENT NO. 6,557,540

REFERENCES

1. J. A. Tennant, Rao, H. S., and Powell, J. David, "Engine characterization and optimal control," *Proceedings of the IEEE Conference on Decisions and Control* (including the 18th Symposium on Adaptive Processes), Ft. Lauderdale, Fla., Dec. 12–14, 1979. IEEE 79CH 7486-OCS, vol. 1, pp. 114–119.
2. Itshak Glaser and Powell, J. David, "Optimal closed-loop spark control of an automotive engine," SAE Paper No. 810058, Society of Automotive Engineers Inc., Warrendale, Pa.
3. Anders Unger and Smith, Kent, "Second-generation on-board diagnostics," *Automotive Engineering* vol. 102, no. 1, Jan. 1994, pp. 107–111.
4. William J. Fleming, "Automotive torque measurement: a summary of seven different methods," *IEEE Transactions on Vehicular Technology,* VT-31, No. 3, Aug. 1982, pp. 117–124.
5. William J. Fleming and Wood, P. W., "Non-contact miniature torque sensor for automotive applications," SAE Paper No. 820206.
6. Yutaka Nonomura; Sugiyama, Jun; Tsukado, Koja; Masahoru, Takeuchi; Itoh, Koji; and Konami, Toshiaki; "Measurements of engine torque with the intra-bearing torque sensor," SAE Paper No. 87042.
7. G. W. Pratt Jr., "An opto-electronic torquemeter for engine control," SAE Paper No. 760007.
8. Charles D. Hoyt, "DC excited capacitive shaft position transducer," U.S. Patent No. 4 862 752 Sept. 5, 1989.
9. Hiroki Kusakabe; Okauchi, Tohru; and Takigawa, Masuo; "A cylinder pressure sensor for internal combustion engine," SAE Paper No. 92071.
10. Stephen J. Citron and Orter, Kevin C., "On-line engine torque measurement utilizing crankshaft speed fluctuations," SAE Paper No. 850496.
11. Clarence E. Kincaid, "Computerized diagnostics for Cummins engines," *Proceedings of Convergence '84,* IEEE '84 CH 1988–5.

ABOUT THE AUTHOR

For biographical information on William G. Wolber, see Chap. 8.

PETITIONER'S EXHIBIT 1002
US PATENT NO. 6,557,540

CHAPTER 10
ACTUATORS

Klaus Müller
Manager, Development of Magnet Valves, Pressure Supply
Automotive Equipment Division 1
Robert Bosch GmbH, Stuttgart

10.1 PREFACE

10.1.1 Introductory Remarks

Numerous open- and closed-loop control systems find application in modern production vehicles, where they provide improved operating characteristics together with enhanced safety, comfort, and environmental compatibility.

The actuators respond to position commands from the electronic control unit to regulate energy, mass, and volume flows.

10.1.2 Actuators: Basic Design and Operating Principles

Conventional final-control elements (standard and spool valves, etc.) have been familiar for some time. A provision for electronic control is required for actuator applications in modern vehicles. The actuator consists of a transformer to convert the input signal from the control unit into (usually) mechanical output quantities, and the conventional final-control element which it governs. (See Fig. 10.1.)

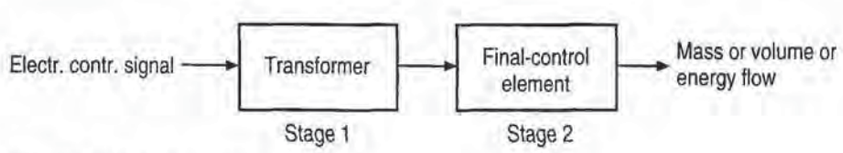


FIGURE 10.1 Basic actuator elements.

Either the control unit or the actuator itself will feature an integral electronic output amplifier. The energy conversion principles (stage 1) determine the classification of the actuators. Electromechanical actuators will also be discussed in the following pages.

ENGR & MATH SCI LIBRARY

PETITIONER'S EXHIBIT 1002
US PATENT NO. 6,557,540

10.2 TYPES OF ELECTROMECHANICAL ACTUATORS

10.2.1 Magnetic Actuators

dc Solenoids

Actuator Principles. In order to operate, actuators depend on the forces found at the interfaces in a coil-generated magnetic field when current passes through it. The solenoid actuation force F_m is calculated as

$$F_m = \frac{A\,B^2}{2\,\mu_o} \tag{10.1}$$

where A = pole face area
B = magnetic induction
μ_o = permeability constant ($\mu_o = 4\,\pi\,10^{-7}$ Vs/Am)

On the flat-armature solenoid illustrated in Fig. 10.2*a*, the total solenoid force is 2 F_m. Equation (10.1) can also be applied to versions equipped with a permanent magnet (Fig. 10.2*b*). A particular solenoid force is specified for each technical application. The pole face area, the magnetic circuit, and the coil are then determined for this force.

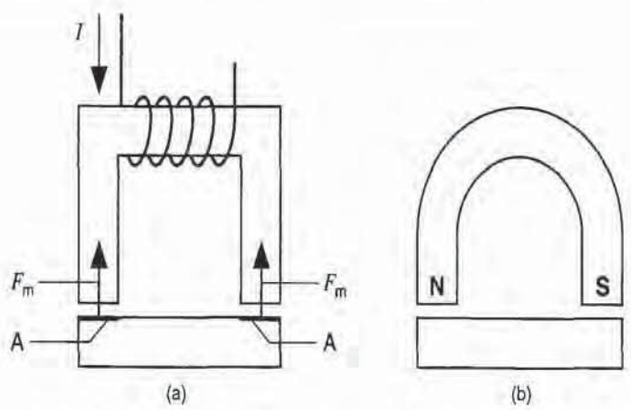


FIGURE 10.2 Flat-armature solenoid featuring field excitation (*a*) via coil; (*b*) via permanent magnet.

Determining Magnetic Circuit and Coil Specifications. The magnetic circuit consists of the working gap (between the armature and the base) and the ferrous regions. Permeability in iron is approximately three orders of magnitude greater than in air. For this reason, the iron regions conduct the field. If the effects of leakage flux are discounted, the absence of magnetic charge, $\oint\!\!\oint B\,dA = 0$, means that the magnetic flux Φ_m remains constant for all cross sections A in the magnetic circuit:

$$\Phi_m = \iint_{A_1} B\,dA_1 = \iint_{A_2} B\,dA_2 = \iint_{A_i} B\,dA_i = \text{const.} \tag{10.2}$$

If the magnetic induction is assumed to be homogeneous for all cross sections A_i, then Eq. (10.2) can be simplified to:

$$\Phi_m = B_1\,A_1 = B_2\,A_2 = B_i\,A_i = \text{const.} \tag{10.3}$$

PETITIONER'S EXHIBIT 1002
US PATENT NO. 6,557,540

The induction lines run at a 90° angle to the surfaces A_i. Equation (10.3) defines the magnetic induction in each section of the magnetic circuit (Fig. 10.3). If, as an example, Index 1 is assigned to the gap section, then B_1 and A_1 are derived with the assistance of Eq. (10.1), and one can proceed to calculate B_i for the other sections.

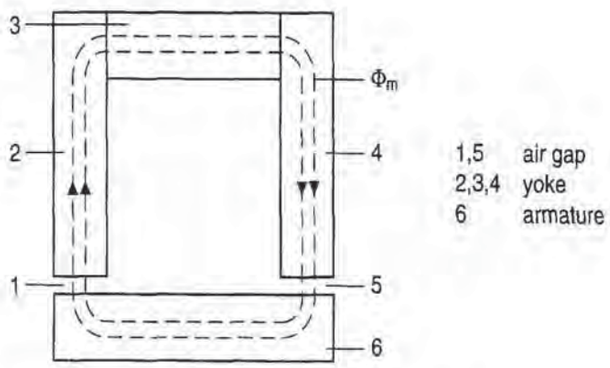


FIGURE 10.3 Magnetic circuit divided into individual sections.

The magnitude of the magnetic field strength $\mathbf{H}_i$ is determined by the material properties (permeability μ_{ri}) of the section in question. Field strength $\mathbf{H}_i$:

$$\mathbf{B}_i = \mu_o \mu_{ri} \mathbf{H}_i \tag{10.4}$$

In air, $\mu_r = 1$. In ferromagnetic materials, μ_r does not remain constant. Rather, it varies as a function of the magnetic field strength **H** (see Fig. 10.4). The relationship between **B** and **H** is defined by the **B-H**-curve.

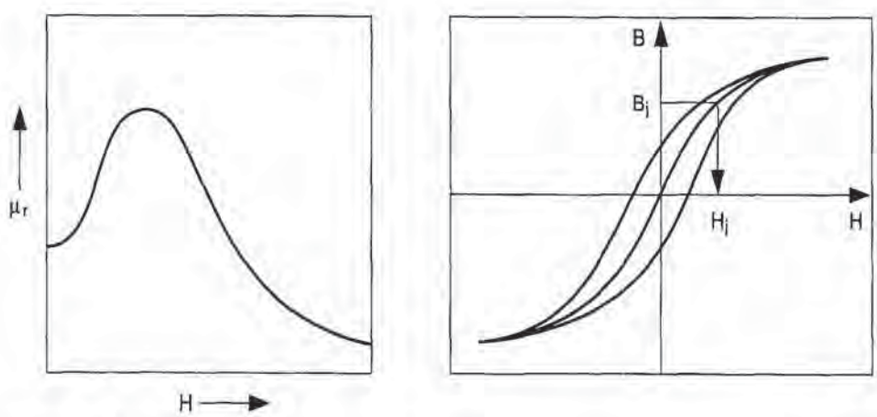


FIGURE 10.4 Progression of permeability and **B-H** curve.

Using the magnetic voltage $V_{mi} = \int \mathbf{H}_i \, d\mathbf{s}$ for the individual section, it is possible to calculate the peripheral magnetic voltage as the sum of the individual magnetic voltages V_{mi}. According to Ampere's law,

$$\Theta = \int \mathbf{H} \, d\mathbf{s} \tag{10.5}$$

this magnetic peripheral voltage is equal to the magnetomotive force Θ. It defines the *total current* of the coil, $\Theta = I\,w$. (I = current, w = number of windings.)

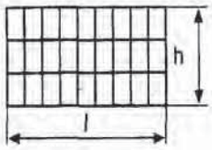
ENGR & MATH SCI LIBRARY UNIV.

PETITIONER'S EXHIBIT 1002
US PATENT NO. 6,557,540

Because the preceding calculation fails to consider leakage flux, the results must frequently be treated as approximations only. It is possible to increase the precision of the calculations by portraying the magnetic circuit as a general network (with gaps and iron regions as reluctance elements) instead of as a series circuit. The results will then reflect the effects of a large proportion of the leakage flux. Maximum precision is achieved with numeric field calculations, which provide numerical solution of Maxwell's equations.

After magnetomotive force Θ has been determined, the field coil must be dimensioned to produce the required magnetic field. The formulas contained in Fig. 10.5 can be employed to determine the field coil's specifications. For a graphic interpretation, see Fig. 10.6.

$A_W = h \cdot l$



Winding cross section area:

$$A_W = \frac{R\,\pi\,\rho\,(d_a+d_i)(1+\alpha\,\Delta\vartheta)^2\,\Theta^2}{2\,k_W\,U^2}$$

Winding number:

$$w = \left(\frac{2\,A_W\,k_W\,R}{\Pi\,\rho\,(d_a+d_i)}\right)^{1/2}$$

Wire diameter:

$$d = \left(\frac{8\,\rho\,(d_a+d_i)\,A_W\,k_W}{\pi\,R}\right)^{1/4}$$

A_W	Winding cross section area	$\Delta\vartheta$	Temperature differential between coil and room temperature
R	Coil resistance	Θ	Magnetomotive force
ρ	Specific resistance of coil wire	k_W	Coil space factor (ratio of total wire area (w/o insulation) to winding cross section area)
d_a	Outer diameter of windings	U	Voltage at coil
d_i	Inside diameter of windings		
α	Thermal resistivity coefficient of coil wire		

FIGURE 10.5 Determining coil data for specified coil resistance and voltage levels.

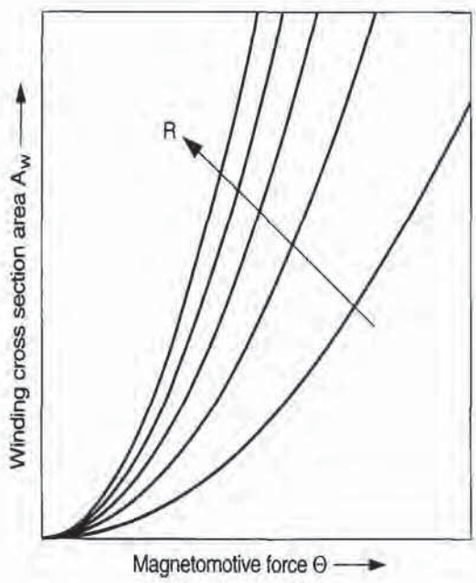


FIGURE 10.6 Area of winding A_w as function of magnetomotive force Θ (parameter coil resistance).

PETITIONER'S EXHIBIT 1002
US PATENT NO. 6,557,540

To minimize the size of the solenoid assembly, the magnetic circuit and the coil must be dimensioned to produce the smallest overall size. The formulas for coil dimensions (Fig. 10.7) can be used to minimize the volume of pot-shaped solenoids.

$$\frac{l}{d} \approx 1.5 \qquad \frac{h}{d} \approx 0.4 \ldots 0.5$$

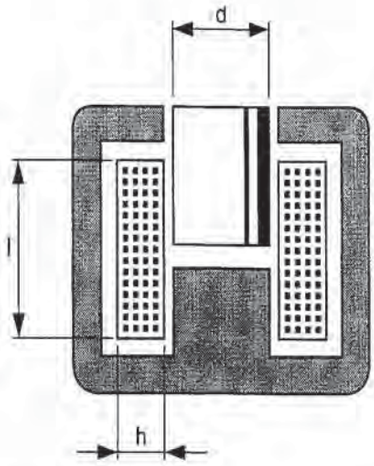


FIGURE 10.7 Selecting coil dimensions for pot-shaped solenoids.

In general, the solenoid is iteratively optimized by changing geometry in those critical areas within the magnetic circuit requiring a high magnetic voltage V_{mi}. The magnetomotive force Θ is then recalculated for the modified magnetic circuit. Figure 10.8 shows the optimization of solenoid diameter D for a particular armature diameter d.

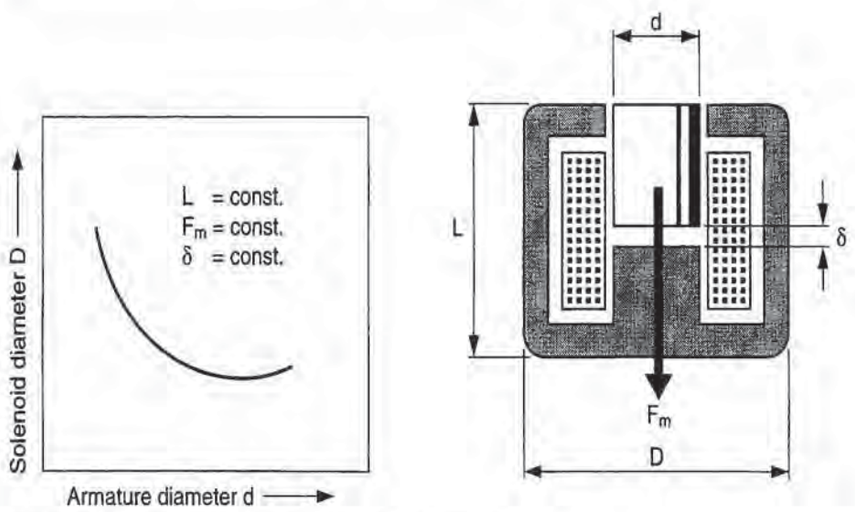


FIGURE 10.8 Relationship between solenoid and armature diameters.

Magnetic Force Curve. When the unit is intended for use in an actuator, the relationship between magnetic force and stroke will be required. With a flat armature and base, and without including the iron regions, Ampere's law [Eq. (10.5)] and Eq. (10.4) provide the following:

$$\Theta = H_\delta \delta = \frac{B_\delta \delta}{\mu_o} \tag{10.6}$$

where δ = working gap

ENGR & MATH SCI LIBRARY

PETITIONER'S EXHIBIT 1002
US PATENT NO. 6,557,540

Together with the force relationship, Eq. (10.1), the following result is obtained:

$$F_m = \frac{\Theta^2 \mu_0 A_1}{2\delta^2}, \text{ i.e., } F_m \sim \frac{1}{\delta^2} \tag{10.7}$$

The substantial drop in magnetic force will be undesirable in many applications. Modifications to the curve for magnetic force versus stroke represent an alternative to increases in solenoid dimensions. This expedient can be effected through control of the current in the coil or by means of design modifications to the armature and base (see Fig. 10.9).

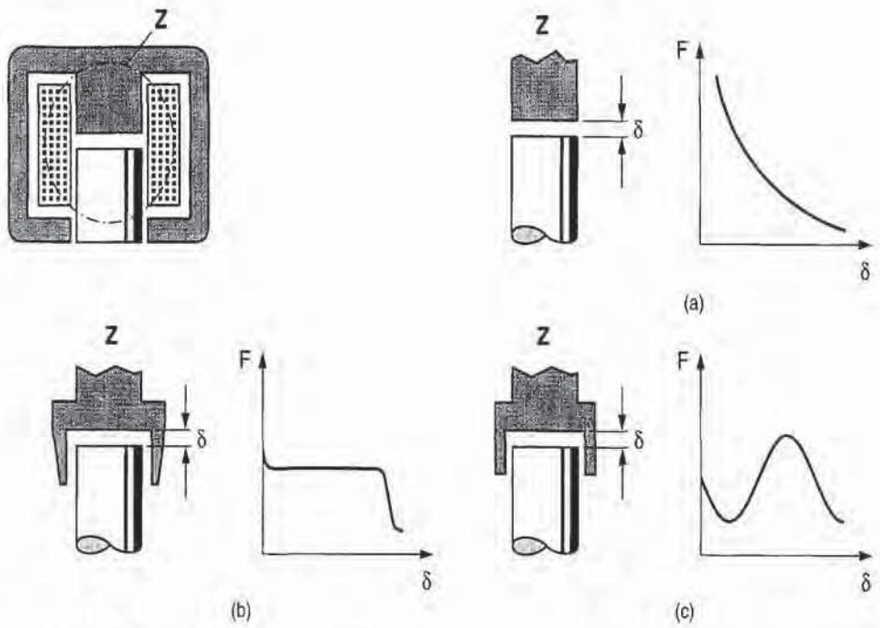


FIGURE 10.9 Design modifications and force curve.

The areas below the force-travel curves, a measure of the work performed, are always the same.

$$\int_0^\infty F_m(\delta)\, d\delta = \text{const.} \tag{10.8}$$

$$\text{with} \quad I = \text{const.}$$

Configuration c can be employed together with a spring to produce a proportional solenoid in which armature travel can be regulated as a function of current. This type of system is sensitive to interference from extraneous factors such as mechanical friction, and hydraulic and pneumatic forces. Thus, final-control systems for high-precision applications must also incorporate a position sensor and a controller (Fig. 10.10).

Dynamic Response. To show the dynamic response pattern more clearly, Fig. 10.11 provides a schematic illustration of the progression over time of three parameters: voltage u at the excitation coil, excitation current i, and armature position s.

The dynamic response pattern can be calculated using computer programs that apply Maxwell's equations (field propagation with eddy currents, self-induction) in conjunction with the motion equation.

Approximation formulas can be employed to derive rapid estimates (eddy currents and magnetic resistance in the iron regions are not taken into account):

PETITIONER'S EXHIBIT 1002
US PATENT NO. 6,557,540

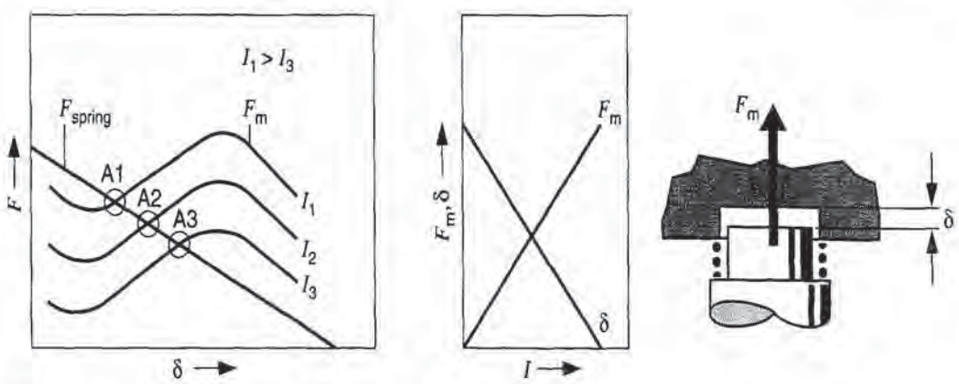


FIGURE 10.10 Operating points of a proportional solenoid.

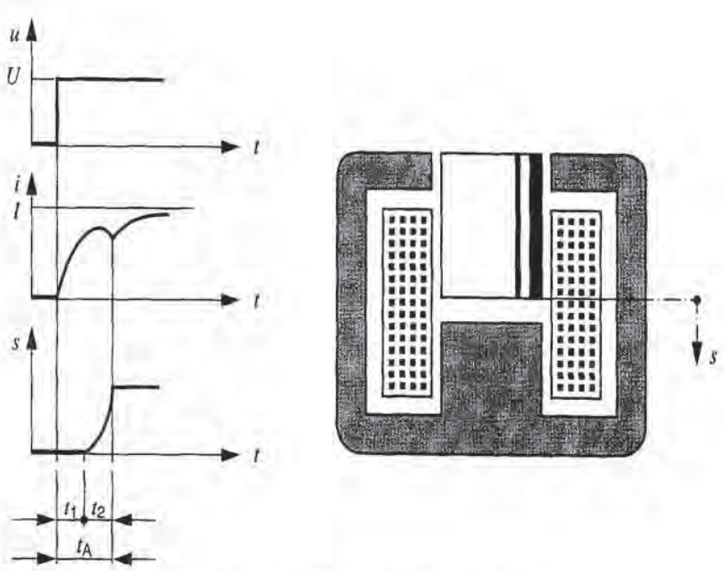


FIGURE 10.11 Progression of voltage, current, and armature travel.

$$t_1 \approx \frac{L_o}{R} \ln \frac{1}{1 - \frac{R}{U}\left(\frac{2 F_{mech}\, \delta_o}{L_o}\right)^{1/2}} \tag{10.9a}$$

$$t_2 \approx \left(\frac{3\, \delta_o m}{U\left(\frac{F_{mech}}{2\, \delta_o L_o}\right)^{1/2} - R\frac{F_{mech}}{L_o}}\right)^{1/3} \tag{10.9b}$$

where L_o = initial inductance
R = coil resistance
U = voltage at solenoid
δ_o = gap with armature lowered
F_{mech} = armature counterforce (treated as constant)
and t_1, t_2, see Fig. 10.11

ENGR & MATH SCI LIBRARY

PETITIONER'S EXHIBIT 1002
US PATENT NO. 6,557,540

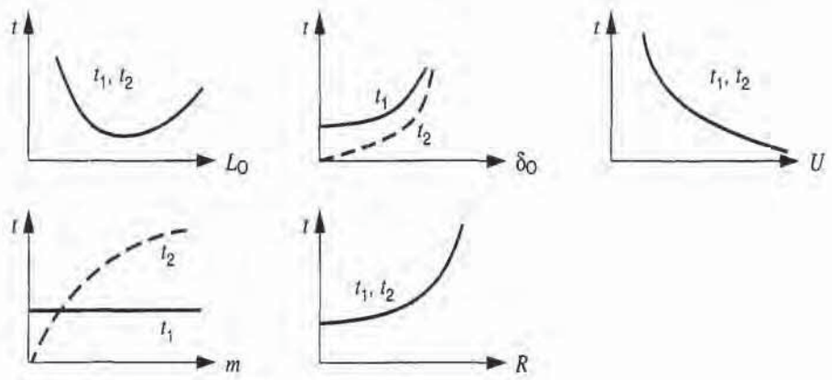


FIGURE 10.12 Relationships of t_1 and t_2.

Figure 10.12 provides an overview of the relationships between t_1 and t_2 and the parameters.

The eddy currents must also be considered in calculations dealing with electromagnets intended for operation at high speeds or switching frequencies. When the excitation current is applied suddenly, the progress over time for the magnetic force is

$$F_m(t) = F_{m0}(1 - e^{-t/\tau})^2 \qquad \text{for field generation}$$

and

$$F_m(t) = F_{m0}\, e^{-2t/\tau} \qquad \text{for field dissipation}$$

with

$$\tau = \frac{\mu_0 l_{Fe} ab}{\pi^2 \rho \delta (a/b + b/a)} \qquad \text{for rectangular cross sections}$$

with

$$\tau = \frac{\mu_0 l_{Fe} d^2}{4(2.405)^2 \rho \delta} \qquad \text{for circular cross sections}$$

where F_{m0} = static solenoid force according to Eq. (10.1)
t = time
l_{Fe} = length of iron core in which eddy currents occur
a/b = height/width of iron core (rectangular cross section)
d = diameter of iron core (circular cross section)
ρ = specific resistance
δ = working gap

Lamination to inhibit eddy currents in dc solenoids is not a standard procedure; its application is restricted to extreme cases.

Figures 10.6 and 10.12 illustrate the fact that at a given voltage, small coil resistances will furnish a small coil and short activation times. However, these benefits are accompanied by a simultaneous increase in the power loss $P_v = U^2/R$. The coil is thus designed to operate at the maximum permissible temperature.

Torque Motors. The torque motor consists of a stator and an armature—both made of soft magnetic material—and a permanent magnet. The pivoting armature can be equipped with either one or two coils.

Figure 10.13*a* shows only the magnetic flux generated by the permanent magnet. The armature is resting at the center position. The magnitude of the magnetic induction is the same at all

PETITIONER'S EXHIBIT 1002
US PATENT NO. 6,557,540

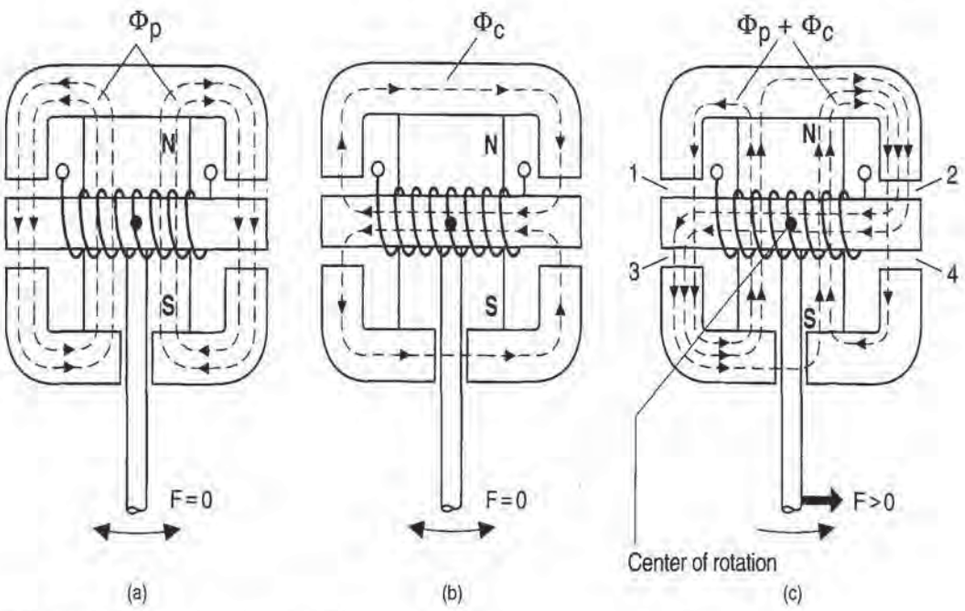


FIGURE 10.13 Design and operation of the torque motor.

gaps. Because equal amounts of force are generated at the armature ends, the forces acting on it exercise a mutual canceling effect.

Figure 10.13*b* illustrates only that magnetic flux which is generated at the coil. Figure 10.13*c* shows the cumulative pattern for the fluxes from *a* and *b*, with increased flow at gaps 2 and 3 ($\Phi_p/2 + \Phi_c/2$) accompanied by reductions at gaps 1 and 4 ($\Phi_p/2 - \Phi_c/2$). Using Eq. (10.1), the torque in the center position is

$$M = F_m r = \frac{r A B_p}{2 s} w I, \text{ i.e., } M \sim I \tag{10.10}$$

where r = armature radius
A = pole face area
B_p = magnetic induction in gap generated by permanent magnet
s = length of gap
w = number of coil windings
I = current.

Torque motors are used for applications in which substantial forces are required over small operating angles. They react more rapidly than electromagnets. In hydraulic and pneumatic applications, torque motors deliver good performance as drive units for flapper and nozzle systems.

Electromagnetic Step Motors. Electromagnetic step motors are drive elements in which a special design operates in conjunction with pulse-shaped control signals to carry out rotary or linear stepped movements. Thus, one complete rotation of the motor shaft will be composed of a precisely defined number of increments, step angles ϕ_0. The magnitude of these angles is determined by the phase number q, the pole pair number p, and by the number of teeth z in the step motor. The step motor is thus capable of transforming digital control signals directly into discontinuous rotary motion. In principle, the step motor is essentially a combination of dc solenoids. The calculations employed for dc solenoids are thus also suitable for application with electromagnetic step motors. Depending upon the configuration of the magnetic circuit, a distinction is made between three types of step motors: the variable-reluctance step motor (neutral magnetic circuit), heteropolar units (polarized magnetic circuit), and hybrid devices.

ENGR & MATH SCI LIBRARY

PETITIONER'S EXHIBIT 1002
US PATENT NO. 6,557,540

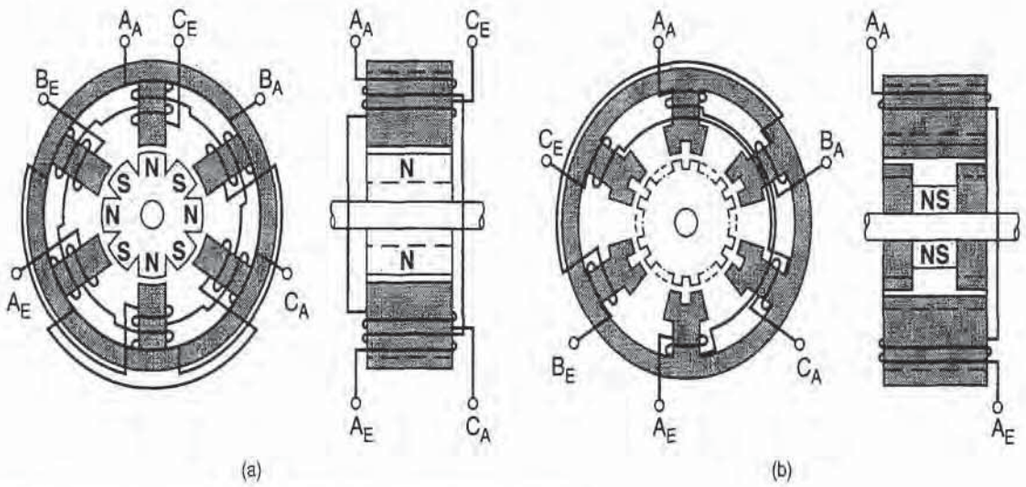


FIGURE 10.14 (*a*) Heteropolar step motor and (*b*) hybrid step motor.

Due to its positive operating characteristics (holding force available in power-off state, improved cushioning, lower control power requirement for a given volume), the polarized step motor has come to be the most widely applied (see Fig. 10.14).

Drive systems featuring electromagnetic step motors combine the following characteristics:

- Field forces induce controllable, incremental movements (minimal wear).
- Precisely graduated movements can be generated using an open-loop control circuit (without position monitors or feedback signals).
- High torque remains available at low angular velocities and in single-step operation.
- Brushless motor design makes it possible to create drive systems which combine reliability with long service life.

The operating characteristics of the rotational step motor can be described with the aid of a stationary torque-angle (M-ϕ) curve. A reasonable approximation can be obtained using sinus-shaped curves with a phase displacement reflecting the switching states of the phase windings (A, B, C) (Fig. 10.15*a*). Assuming that external torque inputs can be excluded, the

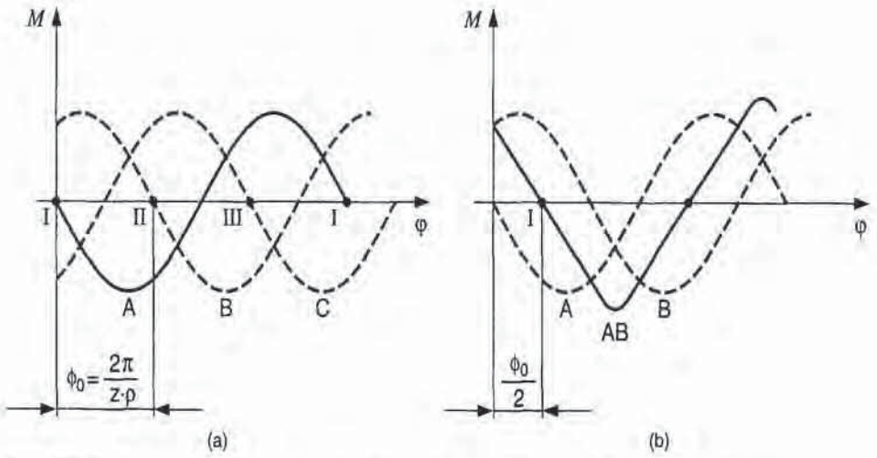


FIGURE 10.15 (*a*) Stationary torque-angle characteristics and (*b*) step-halved.

PETITIONER'S EXHIBIT 1002
US PATENT NO. 6,557,540

armature's stable position will be found where the backslope of the curve intersects the abscissa ($I, \Sigma M = 0, dM/d\phi < 0$). Phase B, C, etc., can then be activated to perpetuate rotation. The periodicity of the stable positions I, II, III is the step angle ϕ_0.

If phase A is followed by simultaneous excitation of A and B with current pulses of the same amplitude, the result is a summing pattern corresponding to Fig. 10.15*b*. The geometric step angle ϕ_0 can then be halved. Alternatively, simultaneous excitation with current pulses of different amplitudes (current control) can be used to subdivide ϕ_0 to almost any degree desired (microstep operation). However, the use of this strategy to enhance the step motor's positioning precision is not possible due to manufacturing tolerances. When step motors are used in drive systems which rely upon open-loop control methods, avoiding stepping errors becomes an important priority (synchronous response).

For critical applications, dynamic simulation of the step drive system's dynamic response pattern is recommended. Here, a good approximation is derived by portraying the step motor using a transfer function of a second-order system. Dynamic response can also be evaluated using the torque-step frequency pattern (*M-f* pattern) for potential step-error-free operation in a start-stop frequency range, Fig. 10.16*a*, and an operating frequency range, Fig. 10.16*b*.

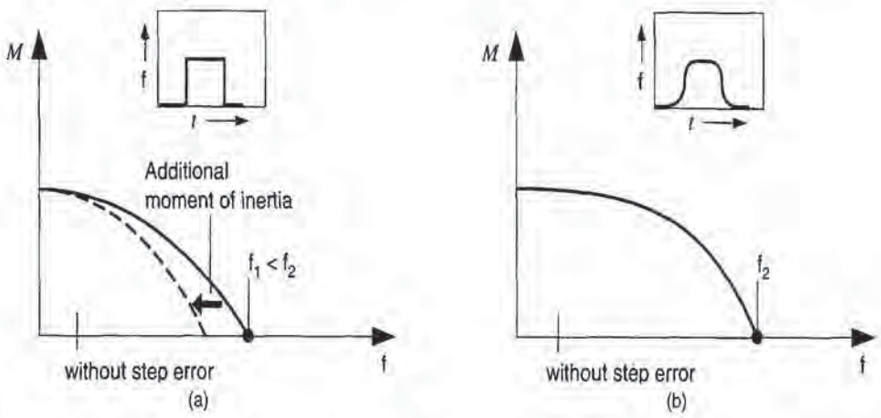


FIGURE 10.16 Torque-step frequency characteristic.

The range in which step error does not occur contracts in response to additional inertial torques or mobile masses. Impressed current induces an upward shift in the potential frequency range which is larger than that derived from impressed voltage. This demonstrates that the step motor's response pattern is strongly influenced by the electronic control strategy. The stepping frequency controls the angular velocity, the pulse distribution (A → B or A → C, see Fig. 10.15) determines the direction of rotation, and the number of pulses governs the pivot angle.

Step motors are only suitable for use as direct-drive elements (the motor's armature operates directly against the actuated unit, no gear drive) in those applications where the influence of load fluctuations and interference factors remains limited, as stepping errors can otherwise occur. For this reason, digital linear actuators featuring integrated rotary step motors and threaded spindles are becoming increasingly popular as linear-motion generators in high-demand applications. When operated within a closed-loop control system, step motors can provide improvements in dynamics, positioning precision, and sturdiness. However, the cost advantages associated with open-loop operation are forfeited.

Moving Coils. The moving coil is an electrodynamic device (force applied to current-saturated conductor in a magnetic field). A spring-mounted coil is located in the ring gap of a magnetic circuit featuring a permanent magnet. When current flows through the coil, a force is exerted against it. The direction of this force is determined by the flow direction of the current itself.

ENGR & MATH SCI LIBRARY

PETITIONER'S EXHIBIT 1002
US PATENT NO. 6,557,540

The positioning force can be calculated using

$$F = B_A L_W I, \text{ i.e., } F \sim I \tag{10.11}$$

where B_A = magnetic induction in the gap
L_W = length of the coil wire
I = excitation current

As the force is not affected by the travel position, a spring can be included to produce a proportional relationship between travel and current.

The advantages of the moving coil include low hysteresis and good linear response. Low mass acts in combination with low coil inductance to provide excellent dynamic-response characteristics. The main liabilities of this design lie in the low force and limited work per stroke for any given unit dimensions.

dc Motors. dc motors are used to discharge a multiplicity of functions in modern cars (today up to 70 motors per vehicle). These motors are generally permanently excited dc devices, as the magnetic field remains continually available without additional energy consumption. For economic reasons, these units are virtually always equipped with ferrite magnets.

Design and Operation. The dc motor depends for its operation on the forces generated in a conductor within a magnetic field when current is applied.

The permanent-magnet-excited motor consists of

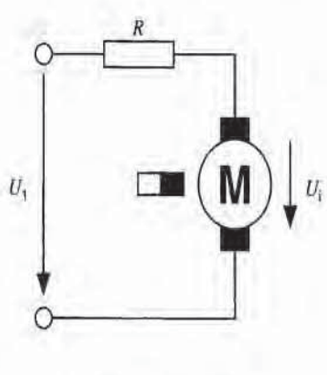
- The magnetic circuit consisting of a permanent magnet for generation and an iron core and a stator frame to conduct the magnetic flux
- Energized coils
- Carbon brushes and commutator, arranged to direct the current to the rotating coil while maintaining the force flow in a single direction

The stationary characteristic can be represented using the following equations (see Fig. 10.17).

$$U_1 = IR + U_i \tag{10.12a}$$

$$U_i = c\, z\, \Phi\, \omega \tag{10.12b}$$

$$M_i = M_v + M = c\, z\, \Phi\, I \tag{10.12c}$$



U_1 – Terminal voltage
U_i – Induction voltage
M – Shaft torque
M_a – Starting torque
M_i – Internal torque
M_v – Torque loss
c – Constant
z – Number of conductors
Φ – Magnetic flux
ω – Armature rotation frequency
I – Current
R – Armature resistance

FIGURE 10.17 dc motor, circuit diagram.

PETITIONER'S EXHIBIT 1002
US PATENT NO. 6,557,540

After inserting Eqs. (10.12*b*) and (10.12*c*) in (10.12*a*), with

$$\omega_{0i} = \frac{U_1}{c\, z\, \Phi} \qquad \text{(ideal idle speed)} \tag{10.13a}$$

$$M_a = c\, z\, \Phi\, \frac{U_1}{R} - M_v \qquad \text{(stall torque)} \tag{10.13b}$$

one obtains

$$\omega = \omega_{0i}\left(1 - \frac{M + M_v}{M_a + M_v}\right) \tag{10.14}$$

or, with idle speed $\omega_0 = \omega(M = 0)$

$$\omega = \omega_0\left(1 - \frac{M}{M_a}\right) \tag{10.15}$$

The motor draws power P_1 from the dc circuit.

$$P_1 = U_1 I \tag{10.16}$$

or

$$P_1 = \frac{U_1}{c\, z\, \Phi}\,(M_v + M) = \omega_0\,\frac{M_v + M_a}{M_a}\,(M_v + M) \tag{10.17}$$

The output at the shaft is the mechanical power P_2

$$P_2 = M\,\omega = M\,\omega_0\left(1 - \frac{M}{M_a}\right) \tag{10.18}$$

Using Eqs. (10.17) and (10.18), the efficiency η can be calculated as a function of the shaft torque.

$$\eta = \frac{P_2}{P_1} = \frac{M(M - M_a)(M_v + M_a)}{M_a(M_v + M)} \tag{10.19}$$

Maximum efficiency as a function of load is obtained by setting the derivative $d\eta/dM = 0$ with

$$M_{\max} = M_v + [M_v(M_v + M_a)]^{1/2} \tag{10.20}$$

In comparison, the output power derived with Eq. (10.18) reaches a maximum at $M = M_a/2$, and thus at a higher value.

Figure 10.18 shows a performance diagram with speed n, current I, and efficiency η as function of the load torque M. It is not possible to determine speed and current separately.

Equations (10.12*a*) through (10.20) illustrate the interactions and the factors that affect the motor's performance curve. The influence of the design parameters is shown in Fig. 10.19.

The magnetic flux Φ is determined by the dimensions and intrinsic material characteristics of the magnet, and by the stack length of the armature and the rest of the magnetic circuit. The speed/torque curve responds to increasing magnetic flux Φ by tilting progressively to the horizontal axis; this response pattern is indicative of a more powerful motor (see Fig. 10.19*a*).

Variations in the number of turns z change the idle speed n_o at the same starting torque (see Fig. 10.19*b*); changes in the armature's resistance (produced by selecting a different wire diameter d) affect the stall current, and thus the stall torque, obtained at any given idle speed n_o (see Fig. 10.19*c*). The maximum achievable copper content is determined by the winding technique.

ENGR & MATH SCI LIBRARY

PETITIONER'S EXHIBIT 1002
US PATENT NO. 6,557,540

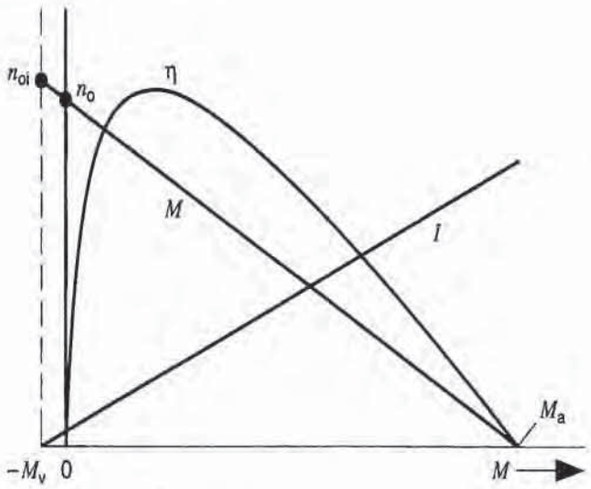


FIGURE 10.18 Motor performance curve.

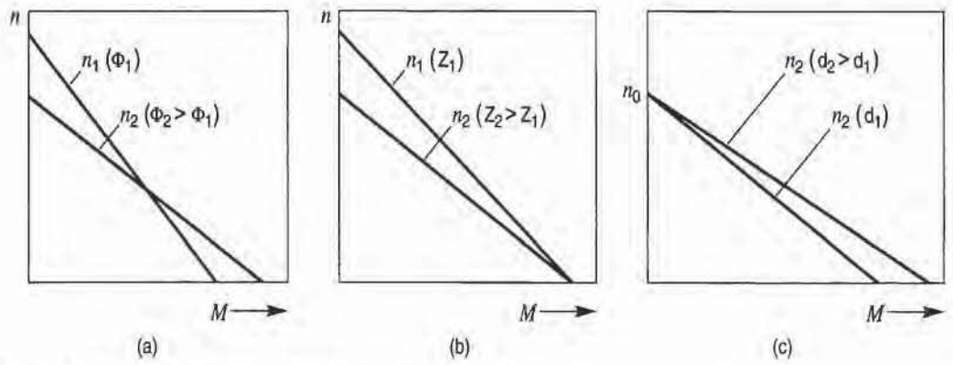


FIGURE 10.19 Effect of design parameters on rotational speed.

Units used in real-world applications display small deviations from the theoretical performance curve as a result of voltage drop at the carbon brushes, the current transfer to the commutator, the armature reaction field produced by the motor's current, and, finally, various rotational and flux losses.

The options for using the electrical parameters to affect the rotating speed are illustrated in Fig. 10.20. Variations in the voltage U (e.g., of the kind produced electronically with a pulse-width modulation) produce a parallel displacement in the speed curve (Fig. 10.20*a*). Other common options include the installation of a ballast resistor R_v and the inclusion of a third carbon brush. Less common (due to cost) is a design in which the winding is divided between two commutators; these can then be activated individually, in parallel, or in series. Servo motors generally operate for brief periods of time, but also over the entire range represented by the unit's characteristic curve.

Each motor must be built specifically for the operating conditions anticipated for the individual vehicle. Ferrite magnets must be selected for the lowest potential temperature, as it is here that the resistance to demagnetization is lowest. When circumstances demand, thermoswitches can also be included to provide protection against overheating.

Automotive actuators must be small and light. Motor volume is directly proportional to torque requirement. At the same time, the power output is proportional to torque multiplied

PETITIONER'S EXHIBIT 1002
US PATENT NO. 6,557,540

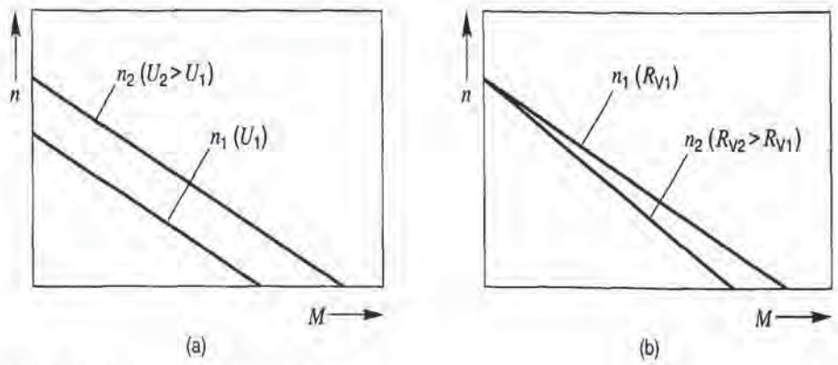


FIGURE 10.20 Speed variations in dc motors.

by rotating speed. Thus, the output can be increased by raising the operating speed; here the accompanying rise in noise levels is the limiting factor. Small motors are equipped with gear-drive units to obtain the required levels of actuating force.

Magnetostrictive Actuators. Ferromagnetic materials respond to increased magnetic field strength by expanding or contracting (magnetostrictive effect). This is due to the Weiss' domains turning in the field direction. The maximum contraction obtained with iron is –8 μm/m. Highly magnetostrictive materials composed of rare-earth/iron alloys display a maximum elongation of 1500 to 2000 μm/m. Maximum potential elongation is obtained at the optimal mechanical pre-tension T_0 (Fig. 10.21).

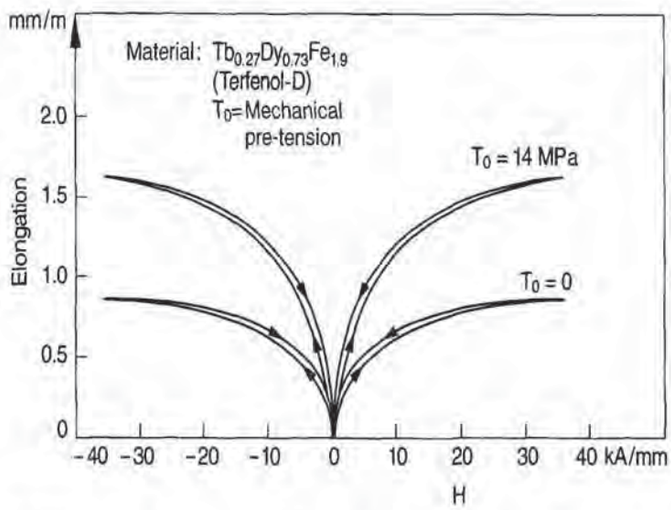


FIGURE 10.21 Magnetostrictive form variations as a function of field strength.

The specific advantages of the magnetostrictive transformer are high actuator forces, rapid response, good rigidity, and a high level of electromechanical efficiency.

The disadvantages include the small variations in length, the high power loss associated with generation of the large maximum field strengths which the unit requires (also in static operation), the length variation with hysteresis, the expense, and the limited availability of the requisite materials. The material is also brittle and difficult to machine.

The commercial availability of the transformers is limited to units designed for research purposes. We are not familiar with any applications in production motor vehicles.

ENGR & MATH SCI LIBRARY

PETITIONER'S EXHIBIT 1002
US PATENT NO. 6,557,540

10.2.2 Electrical Actuators

Piezoelectric Actuators. When mechanical compression and tension are brought to bear on a piezoelectric body, they produce an asymmetrical displacement in the crystal structure and in the charge centers of the affected crystal ions. The result is charge separation. An electric voltage proportional to the mechanical pressure can be measured at the metallic electrodes (direct piezoelectric effect).

If electric voltage is applied to the electrodes on this same body, it will respond with a change in shape; the volume remains constant. This reciprocal piezoelectric effect can be exploited to produce actuators. Sintered ceramics, lead-zirconate-titinate (PZT), are the commonly used materials for these applications. The precise composition can be modified to obtain the desired material characteristics. The magnitude of the shape change depends on the electric field strength E. The relevant equation is $E = U / s$ (U = voltage, s = electrode gap). Single-element actuators require field strengths of up to 2 kV/mm and therefore very high voltage to achieve maximum travel (see Fig. 10.22).

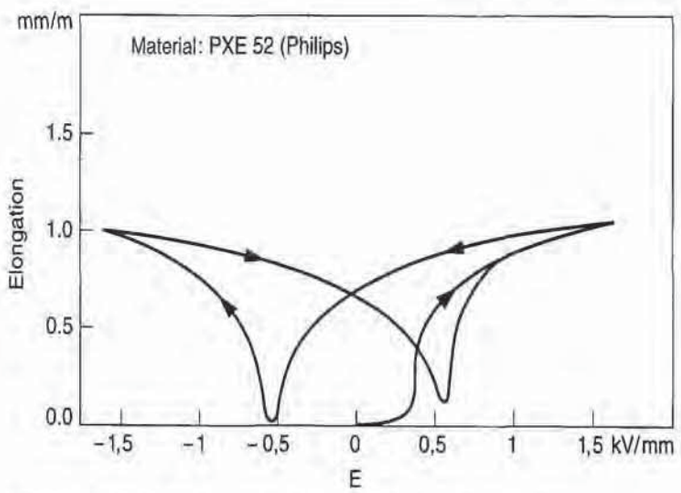


FIGURE 10.22 Form changes as a function of electric field strength.

Stacked-design translational devices consist of piezoelectric layers of between 0.3 and 1 mm in thickness, featuring a metallic electrode between each layer. This design is employed to lower the voltage (down to, for instance, 800 V) while simultaneously increasing the excursion rate. The layers are electrically parallel and form a series circuit (see Fig. 10.23*a*).

Flex elements are formed by joining two layers with varying intrinsic rates of elongation. The elongation occurs along the vertical axis of the direction in which the field strength is projected (transverse effect). Flex elements display larger excursion rates with lower actuating forces (see Fig. 10.23*b*).

New manufacturing techniques make it possible to produce multilayer piezoelectric devices with thinner layers; these can be used to obtain the required field strength at voltages as low as approximately 100 V and below.

However, due to the numerous parallel elements, the advantages associated with the low control voltage are obtained only at the price of increased capacitance and higher operating currents.

The positive attributes of the piezoelectric actuator include a high dynamic response level, substantial actuator force, voltage-proportional elongation, excursion with no power consumption in static operation, and (practically) no wear in the piezoelectric element.

The corresponding liabilities include minimal elongation changes, high operating voltage, hysteresis during elongation, a temperature-sensitive stroke, and a drift in operating response as the unit ages. The material itself is brittle and difficult to machine.

PETITIONER'S EXHIBIT 1002
US PATENT NO. 6,557,540

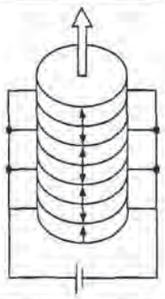
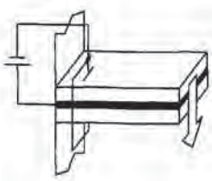
	a	b
Elongation Δl	Parallel to electrical field	Perpendicular to electrical field
Design types		
Typical regulation distance and elongation	$\frac{\Delta l}{l_0} = 0.17\ \%$	$\Delta l \leq 1000\ \mu m$ and more
max. statical load	$\leq$ 35 000 N	$\leq$ 0.01 ... 0.05 N
Typical operation voltage	150 ... 1000 V 50 ... 150 V (multilayer)	10 ... 300 V

FIGURE 10.23 Design and specifications of different transformer versions.

Piezoelectric actuators are applied in precision positioning devices and as active oscillation dampers. Potential automotive applications (with a voltage supply of 12 V) have yet to be thoroughly investigated. However, it is expected that the piezoelectric actuator—and the multilayer stacked-design device in particular—will gain popularity in closed-loop automotive control systems, where they will serve as a replacement for the conventional actuator in applications requiring a higher level of performance.

Electrostatic Actuators. In the past, use of electrical field forces was restricted to some measurement devices and to the acceleration of charged particles. Microactuator technology makes it possible to apply these small forces in mechanical drive devices. These devices combine high switching speeds with much smaller energy loss than that found in electromagnetic actuators. The disadvantages are the force/travel limitations and the high operating voltages. At present, microactuators are rarely encountered outside the research laboratories; thus, the electrostatic actuator's current commercial significance is negligible.

Electrorheological Fluids. The electrorheological effect is based on polarization processes in minute particles suspended in a fluid medium. These particles modify the fluid's viscosity according to the orientation in the electrical field. The effect can be employed to adjust the viscosity between "freely flowing" and "rigid." Reaction times are measured in ms. Among the disadvantages are interference factors, temperature sensitivity, high voltages, control powers of several hundred watts, and the price, which is still high. The electrorheological effect is exploited in controlled transfer and damping elements.

10.2.3 Thermal Actuators

Temperature-Sensitive Bimetallic Elements. The temperature-sensitive bimetallic element is composed of at least two bonded components of varying thermal-expansion coefficients. When heat is applied, the components expand at different rates, causing the bimetallic element to bend. When electrically generated heat is applied, these devices become actuators.

ENGR & MATH SCI LIBRARY UCLA

PETITIONER'S EXHIBIT 1002
US PATENT NO. 6,557,540

The passive component is characterized by a lower thermal-expansion coefficient. Meanwhile, the active component should maintain a constant coefficient of thermal expansion over the largest possible range.

The passive element in the most common type of temperature-sensitive bimetallic device is invar ($FeNi_{36}$), while the active component is an alloy of iron, nickel, and manganese ($FeNi_{20}Mn_6$). Common element configurations include strips, coils, spirals, and wafers. Temperature-sensitive bimetallic devices are readily available and inexpensive. They can be applied at temperatures of up to roughly 650 °C, and display a high degree of consistency in their shape-change response (up to several million cycles). The drawbacks include the modest actuator forces, the low work potential for a given volume (energy density), and the fact that only a single type of shape modification (flexural) is possible.

Memory Alloys. Memory alloys are metallic materials which exhibit a substantial degree of "shape memory." The explanation for this phenomenon can be found in the reversible, thermoelastic martensitic transformation, in which two different crystal structures are adopted. As long as the temperature remains below the transformation threshold, the structure remains martensitic. However, when the alloy is heated beyond the transformation temperature, it responds by becoming austenitic.

The element's shape is changed permanently by the one-way effect. If the element is heated to beyond the transformation temperature, it returns to its former shape. If the component is then reshaped after cooling, the entire process can be repeated. Thermomechanical pretreatment processes can be employed to achieve a two-way effect. The component then assumes one defined shape when heated, and another when cooled.

Yet another phenomenon is superelasticity. Application of loads produces an extension of up to 10 percent; the effect is reversed once the load is removed. However, because this effect is extremely sensitive to temperature, it has yet to be employed in the construction of actuators. The materials are commercially available, the base materials are nickel-titanium (NiTi–) and copper-zinc-aluminum alloys (CuZnAl–). The transformation temperatures of these alloys lie between –100 and +100 °C, with the one-way effect also being obtained outside this range.

The benefits of memory alloys include the high effective output for a given volume and the ability to complete work cycles within a minimal temperature interval of 10 to 30 °C. The memory components can be formed to suit the particular application. The wire's resistance can be employed for direct heating. The material itself can be formed with or without physical machining, and can also be welded. Among the disadvantages must be counted the limited thermal range of application and the high price.

Memory alloys are used as drive, final-control, and triggering elements in various technical applications (automotive, household appliances, heating and climate control, medical technology, etc.). The forms assumed by the actual components include triggering wires, coil springs, and flex and torsion elements.

The memory element can be used as sensor and actuator—for instance, in a liquid medium—in which temperature changes will induce shape changes in the component.

Expansion Elements. The expansion element exploits the volume-versus-temperature response of specific solid and fluid media which exhibit large coefficients of thermal expansion. The volumetric response is converted to a stroke motion. The expansion medium is housed in a rigid container. The motion is converted to a stroke using diaphragms or elastomer inserts. Electrically controlled expansion elements find application as actuators. Expansion elements are inexpensive and robust, and combine large stroke travel with substantial positioning forces.

However, these devices are only suitable for application within a limited temperature range. Their dynamic response is also less than overwhelming. Expansion elements are widely applied in automotive technology (for instance, choke actuators on carbureted engines).

PETITIONER'S EXHIBIT 1002
US PATENT NO. 6,557,540

10.3 AUTOMOTIVE ACTUATORS

10.3.1 Antilock Braking

(See Chap. 15 and **traction control systems**, Chap. 16.)

Both antilock braking systems (ABS) and traction control systems (ASR) limit the rate of slip between tire and road surface. These systems enhance vehicle stability and steering response while maintaining optimal braking and acceleration characteristics. ABS and ASR employ a single set of actuators to modulate braking pressure. In addition, ASR devices supplement braking intervention by adjusting engine output.

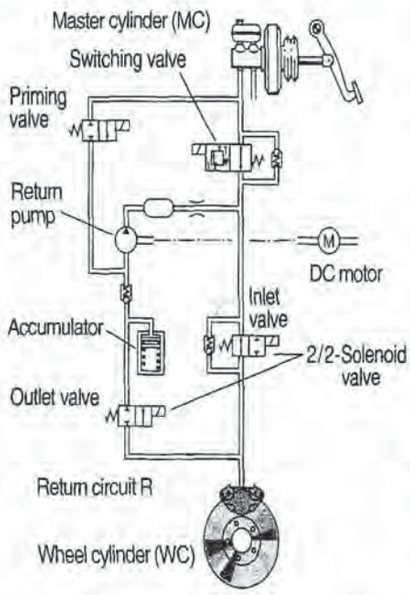


FIGURE 10.24 ABS/ASR hydraulic circuitry.

Actuators for Braking Intervention. Braking pressure is regulated normally via 2/2 solenoid valves (valves with two ports and two switch positions, see Fig. 10.24). When no current is applied, the inlet valve remains open and the outlet valve is closed, allowing unrestricted wheel braking.

ABS/ASR systems modulate pressure by controlling two 2/2 solenoids for each wheel or for two wheels of one axle. With no current, the inlet valve remains open while the outlet valve stays closed. To maintain pressure, current is applied to the inlet valve. Pressure release is obtained by transmitting current to both valves.

Various pulse sequences applied to the inlet valve generate a step-by-step increase of the wheel braking pressure (wheel brake pressure modulation).

Using the same pulse sequence for the outlet valve while the inlet valve remains closed, a step-by-step brake pressure decrease in the wheel cylinders is achieved. Switching and priming valves of a 2/2 type can be incorporated in the circuit to provide the additional functions required for the ASR (Fig. 10.25).

Solenoid Valve Design. One part of the magnetic circuit is located in the hydraulic chamber; here the armature and the pole piece simultaneously serve as valve elements in a design known as the wet solenoid. The solenoid coil and the other part of the magnetic iron circuit are located outside the hydraulic chamber. This design requires the presence of a pressure-resistant sealing element. This element must also be nonmagnetic, in order to ensure that the magnetic flux flows through the working gap and the armature in the desired fashion.

The solenoid circuit is designed to provide reliable switching and pressure maintenance at maximum temperature (maximum coil resistance), minimum voltage, and maximum pressure. At the same time, armature clearance and residual gap must both be adequate to ensure that the valve continues to function at low temperatures (brake-fluid viscosity changes exponentially (by three powers of ten) in the range between –40 and +120 °C). The maximum operating pressures can extend in extreme cases to more than 200 bar. Typical switching times are 4 to 10 ms. Dynamic response is evaluated according to the pressure variation at a specified control pulse. The duty-cycle requirements for ABS are minimal, but ASR switching and priming valves must be capable of 100 percent permanent duty. The maximum cycle numbers correspond to several million actuations.

ENGR & MATH SCI LIBRARY

PETITIONER'S EXHIBIT 1002
US PATENT NO. 6,557,540

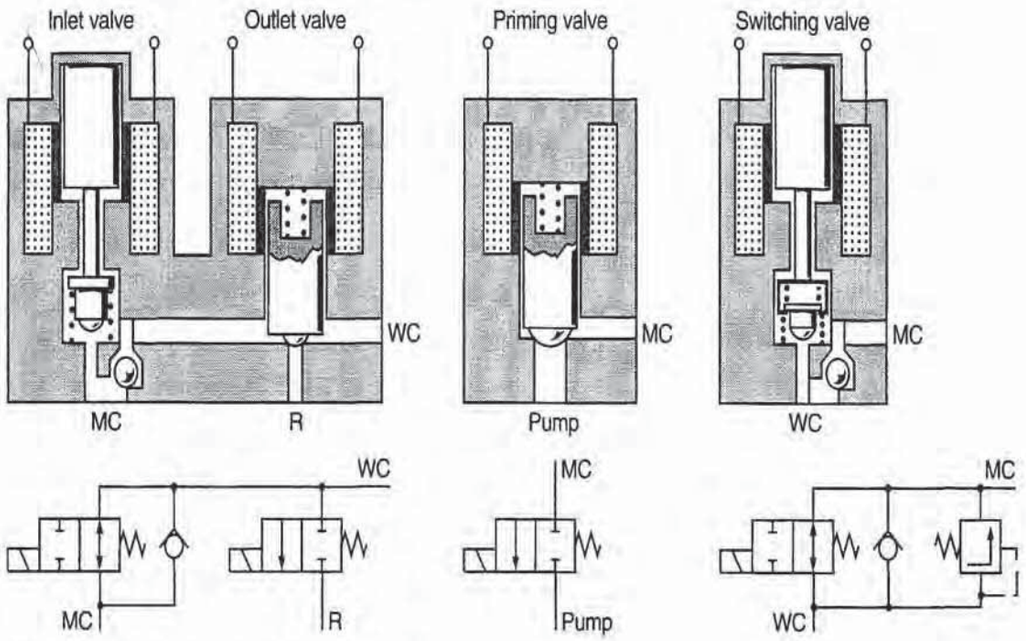


FIGURE 10.25 2/2 solenoid valves for ABS/ASR.

ETC with Throttle-Aperture Adjustment. Either of two standard methods can be employed for throttle regulation. Electronic Throttle Control (ETC) systems feature an actuator (servo motor) mounted directly at the throttle valve. On systems incorporating a traction-control actuator, the actuator (servo motor) is installed in the throttle cable (Bowden cable).

The design configuration of the electronic throttle-control actuator is illustrated in Fig. 10.26. To enhance clarity and facilitate understanding, all rotating components (except the throttle plate) are portrayed as linear-motion devices. The throttle shaft travels between two

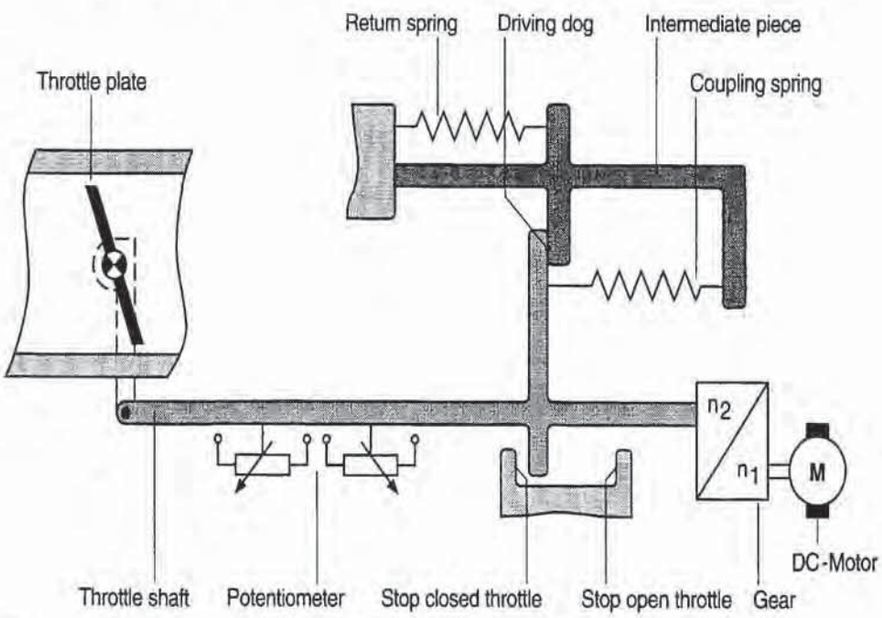


FIGURE 10.26 Operation of electronic throttle control.

PETITIONER'S EXHIBIT 1002
US PATENT NO. 6,557,540

motion limiters; these define the closed throttle and maximum aperture positions. The shaft is powered by a dc motor via a dual-gear drive. When the motor is off, a return spring pulls the intermediate piece back toward the idle-air stop. The driving dog pushes the throttle shaft toward the idle position. The coupling spring holds it in a defined idle position. This position corresponds to an idle speed ensuring adequate engine power to maintain power-steering and brake operation in the event of system failure.

Current can be applied to the dc motor in either direction. One direction opens the throttle plate and tensions the return spring. The other direction closes the throttle plate. When the throttle plate closes all the way, the coupling spring is tensioned. Two potentiometric throttle-position sensors are included in a design calculated to provide redundant system capacity. The electronic control unit uses the signals from these sensors to regulate motor current for the desired throttle position; the signals thus represent part of a closed-loop control system.

Traction-Control Actuator. The actuator can be installed in any of several locations within the engine compartment. No modifications to the throttle body are required.

Figure 10.27 illustrates the operating principles in a simplified linear flow pattern (the actuator components are actually rotary elements). The ends of the Bowden cable sections are connected to rotary cam/linkage spring assemblies.

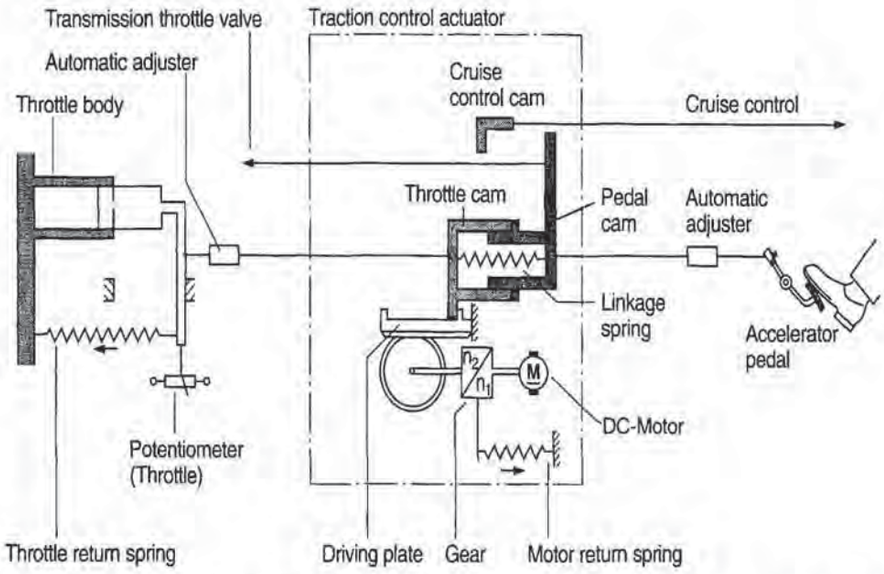


FIGURE 10.27 Operation of a traction-control actuator located between the accelerator pedal and throttle body.

Under normal operating conditions, the pressure applied at the accelerator pedal is relayed through the Bowden cable and linkage spring coupling to open the throttle valve. The servo motor comes to life when the ABS/ASR control unit transmits a command to reduce the throttle-valve aperture. The servo motor pulls the engagement mechanism to the left via gear drive and Bowden cable. Once the initial take-up range has been covered, the linkage is activated to reduce the throttle-valve opening. The servo motor is deactivated as soon as the ASR no longer requires throttle-valve regulation. A return spring then brings the motor back into its original position, allowing the traction control actuator to drive back to its original at rest position.

The traction-control actuator can also be used in conjunction with a cruise-control system. A separate cam connects the Bowden cable for the cruise control to the actuator assembly. This layout is employed to retain the option of traction-control intervention when the cruise-control system is activated.

ENGR & MATH SCI LIBRARY UCLA

PETITIONER'S EXHIBIT 1002
US PATENT NO. 6,557,540

Because the linkage spring must be considerably stronger than the throttle-return spring, it exerts a perceptible effect on the resistance at the accelerator pedal.

Another approach to engine intervention is embodied in a design in which the linkage spring is integrated within the throttle body. Yet a further option is to install a second throttle valve which remains open during normal operation; a separate Bowden cable is installed between this throttle body and the actuator to regulate the valve for active traction-control duties. Because the linkage spring is installed parallel to the throttle-return spring, the preload is substantially lower than that generated by the design described here; there is almost no perceptible feedback at the accelerator pedal. Actuator weight and dimensions are also reduced substantially.

10.3.2 Fuel-Injection for Spark-Ignition Engines

(See Chap. 12.)

Electronically controlled fuel injection systems meter fuel with the assistance of electromagnetic injectors. The injector's opening time determines the discharge of the correct amount of fuel.

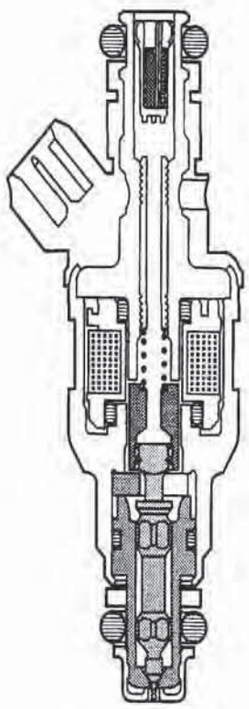


FIGURE 10.28 Injector unit for multipoint fuel injection system.

On single-point injection units, one injector unit is installed at a central location upstream from the throttle valve. Multipoint injection systems feature a separate injector at each cylinder (Fig. 10.28). This type of injector is located in the manifold tract just above the intake port into which it discharges its fuel.

Operating Requirements. The injectors are 2/2 valves with coaxial fuel inlet and lateral plug. They operate with minimal strokes of less than 1/10 mm.

Besides the precise opening and closing, the reliable sealing and the discharge pattern which an individual injector provides are all largely determined by the design of its metering apparatus, thus exercising a major effect on starting and response, fuel consumption, and emissions.

Electromagnetic injectors have to fulfill the demand for precise fuel metering, consistent linear response at minimal quantities, extended dynamic flow range (DFR), good spray formation and atomization, positive seal at injector seat, resistance to corrosion, operating consistency, and low noise.

Low-resistance injectors with current-controlled output stages achieve shorter switching times. See Table 10.1.

10.3.3 Fuel Injection for Diesel Engines

Distributor-Type Fuel Injection Pumps contain rotary solenoid actuators for injection quantity, and two position valves for engine operation and shutoff.

The fuel quantity injected by an in-line pump is a function of control-rack position and pump speed (Fig. 10.29).

PETITIONER'S EXHIBIT 1002
US PATENT NO. 6,557,540

TABLE 10.1 Typical Injector Specifications

	Units	Multipoint injection	Single-point injection
Line pressure . . . max.	kPa	200–380	100–300
Static flow at 250 kPa,	g/min	100–430	—
at 100 kPa,	g/min	—	200–520
Opening time	ms	1.5	0.75
Closing time	ms	0.8	0.65
Variation ratio (DFR)		1:10	1:16
Durability >mio.cycle		1000	1000
Needle/armature weight	g	4.3	2.7
Length	mm	77	53

The control rack of an EDC in-line pump is shifted by a linear-motion solenoid with a conic armature and base for long stroke application (see pages 10.5 and 10.6). The actuator is attached directly to the pump.

When no current is applied to the linear-motion solenoid, a spring pushes the control rack into the stop position and thus interrupts fuel delivery. As current increases, the control-rack travel and, with it the injection quantity, increase.

Typical operating data of the solenoid actuator are (full load, stationary condition): rack travel 13 mm, spring force 32 N, ECU current output 6 A, 200 Hz. By pulsation of the ECU-current, the actuator friction is minimized. Maximum rack travel is about 20 mm.

The electronically controlled unit injector (Fig. 10.30) has been developed to meet the future emissions regulations by realizing high injection pressures and precise control of start of injection and injection quantity.

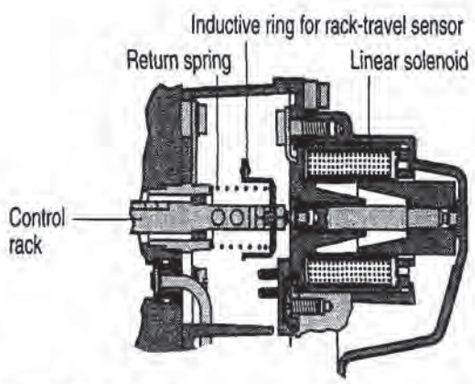


FIGURE 10.29 EDC linear-solenoid actuator.

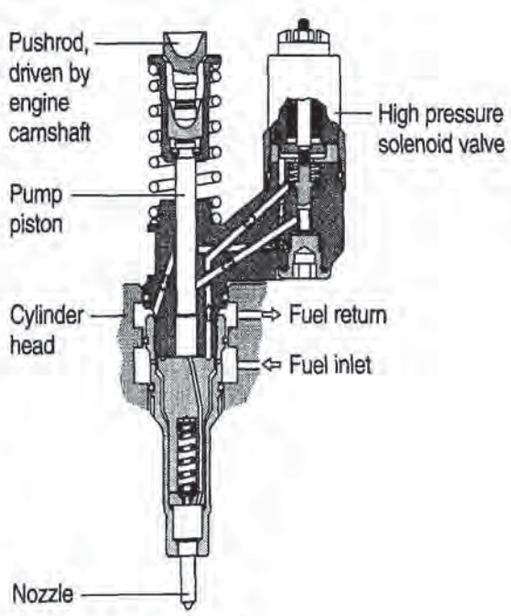


FIGURE 10.30 Unit injector.

ENGR & MATH SCI LIBRARY

PETITIONER'S EXHIBIT 1002
US PATENT NO. 6,557,540

The unit injector combines injection pump and injection nozzle into a single unit, which is installed directly into the engine cylinder head and driven by the engine camshaft. High injection pressures of 1600 bar and more are readily attainable due to low dead volume of compressible fuel.

In order to control start and end of injection, each unit injector contains a time-controlled high-speed solenoid valve. When the valve is open, the unit injector plunger delivers fuel to the low-pressure fuel supply circuit without any injection into the engine cylinder. When the solenoid valve is closed, fuel is delivered to the nozzle for injection into the engine cylinder. Thus, the fuel injection quantity is determined by the time interval between closing and opening of the valve.

Typical switching times for a medium duty/heavy duty truck application are: closing period at rated power, 1000 μs; opening period at rated power, 600 μs. The whole injection process must be completed within a period of about 1 to 2 ms. Consequently, the solenoid-valve motion must occur with an accuracy of less than 10 μs in order to ensure compliance with the usual tolerances for fuel injection quantity and start of injection.

10.3.4 Actuators for Passenger Safety

(See Chap. 24.) Pyrotechnical actuators are used for passenger-restraint systems such as the air bag and the automatic seat belt tensioner. When an accident occurs, the actuators inflate the air bag (or tension the seat belt) at precisely the right instant. Specifications call for the belts to be fully tensioned ~ 10 ms after ignition, while ~ 30 ms are allowed between the ignition point and total inflation for the air bag.

Air bag actuators are available in various sizes, according to vehicle type and application (driver or passenger side), and they are dimensioned to generate gas volumes of between 30 and 200 dm^3. The gases and gas mixtures used for these devices are nontoxic. The section following describes the operating principles for various actuator types.

Pyrotechnical Air Bag Inflator (Gas Generator). Figure 10.31 is an example of a driver-type inflator. When sufficient current is sent through the initiator, or squib, a thin metal filament covered by a sensitive pyrotechnic charge heats up and ignites this charge (Fig. 10.31*a*). The ignition of the squib provides enough energy to light a booster charge, whose combustion

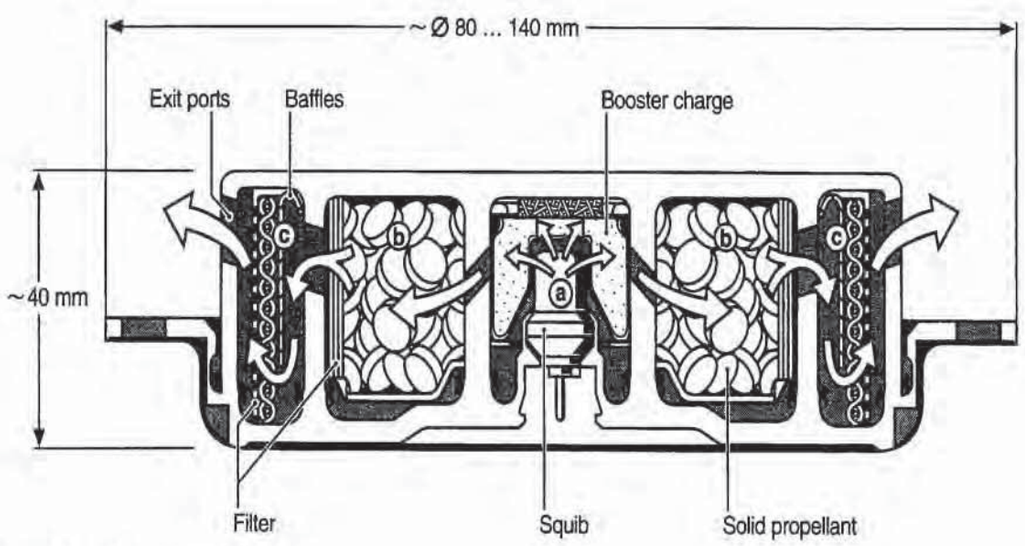


FIGURE 10.31 Gas generator.

PETITIONER'S EXHIBIT 1002
US PATENT NO. 6,557,540

builds up adequate pressure and heat to start the chemical reaction, converting the solid propellant, or gas generant, into gas (Fig. 10.31*b*). The resulting nontoxic hot gas flows over a series of screens, filters, and baffles, cooling down prior to leaving the inflator through exit ports located inside the air bag (Fig. 10.31*c*). The duration of this process is less than one-tenth of a second.

Hybrid (Compressed Gas and Pyrotechnic) Air Bag Inflator. Figure 10.32 is an example of a passenger-type tubular inflator. When sufficient current is sent through the initiator, or squib, a thin metal filament covered by a sensitive pyrotechnic charge heats up and ignites this charge (Fig. 10.32*a*). The ignition of the squib provides enough energy to propel a projectile through a rupture disk, allowing the escape of stored nontoxic compressed gas (Fig. 10.32*b*). The projectile also strikes two primers, lighting a solid pyrotechnic mass, which in turn heats the remaining stored gas (Fig. 10.32*c*). The expanding heated gas flows out of the inflator through exit ports located inside the air bag (Fig. 10.32*d*). The duration of this event is less than one-tenth of a second.

10.3.5 Actuators for Electronic Transmission Control

Continuous operation actuators are used to modulate pressure, while switching actuators function as supply and discharge valves for shift-point control.

In automatic transmissions, response times of 2 ms must be ensured in circuits with flow diameters of up to 2.4 mm, carrying up to 4 dm^3 per minute at a differential pressure of 200 kPa, all within a temperature range extending from –40 to 150 °C; pressure can increase up to 2000 kPa.

On/Off Solenoids. Various versions of the on/off solenoid valve are in use (two-port, three-port, open base state, closed base state). These valves are normally employed for shifting gears, but can also serve in special applications such as control of converter lockup mechanisms or reverse lockouts. Substantial weight savings can be obtained from the use of plastics. On/off valves are controlled through basic switching output stages. Peak-and-hold control strategies can provide weight and size savings.

Variable-Pressure Solenoids (Pressure Regulators). Pressure regulation must remain precise during switching operations and when holding line pressure. Here, analog valves have

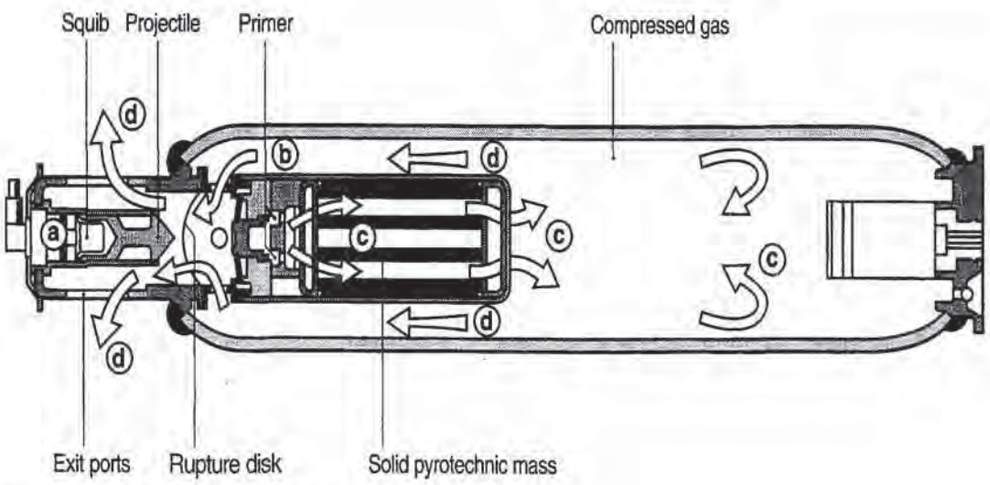


FIGURE 10.32 Hybrid air bag inflator.

ENGR & MATH SCI LIBRARY UCLA

PETITIONER'S EXHIBIT 1002
US PATENT NO. 6,557,540